UNIVERSITY OF OKLAHOMA

GRADUATE COLLEGE

PREPARATION OF FIELD VALIDATION FOR AN ALL-DIGITAL, PERMANENT DOWNHOLE PRESSURE SENSOR DESIGN

A THESIS

SUBMITTED TO THE GRADUATE FACULTY

in partial fulfillment of the requirements for the

Degree of

MASTER OF SCIENCE

By

JACKSON BRAUGHT
Norman, Oklahoma
2023

PREPARATION OF FIELD VALIDATION FOR AN ALL-DIGITAL, PERMANENT DOWNHOLE PRESSURE SENSOR DESIGN

A THESIS APPROVED FOR THE
MEWBOURNE SCHOOL OF PETROLEUM AND GEOLOGICAL ENGINEERING

BY THE COMMITTEE CONSISTING OF

Dr. Runar Nygaard, Chair

Dr. Saeed Salehi

Dr. Hamidreza Karami

© Copyright by JACKSON BRAUGHT 2023
All Rights Reserved.

Acknowledgements

First and foremost, I would like to express my greatest gratitude to my supervisor, Dr. Runar Nygaard for his indistinguishable support, teachings, and persistence during my studies. I would also like to express my gratitude Na Yuan for all her support throughout the course of this project. This thesis would not have been possible without either of you.

Secondly, I would like to thank the University of Oklahoma for giving me the opportunity to further my educational and professional dreams with a special thank you to my committee members, Dr. Runar Nygaard (chair), Dr. Saeed Salehi, and Dr. Hamidreza Karami, for their assistance in completing my studies.

Lastly, I would like to thank my family and the rest of my community for their continued support as I have relentlessly pursued my professional dreams.

Disclaimer

This work was sponsored by the United States Department of Energy and National Energy Technology Laboratory (NETL) (Federal Grant Number: DE-FE0031781; project title: All-digital Sensor System for Distributed Downhole Pressure Monitoring in Unconventional Fields). Neither the United States Government nor any agency or contractor thereof, nor any of their employees, makes any warranty, express or implied, or assumes any legal liability or responsibility for the accuracy, completeness, or usefulness of any information, apparatus, product, or process disclosed, or represents that its use would not infringe privately owned rights. Reference herein to any specific commercial product, process, or service by trade name, mark, manufacturer, or otherwise, does not necessarily constitute or imply its endorsement, recommendation, or favoring by the United States Government or any agency or contractor thereof. The views and opinions of authors expressed herein do not necessarily state or reflect those of the United States Government or any agency or contractor thereof.

Table of Contents

List of Figures

List of Tables

Abstract

Downhole pressure sensing has become increasingly important in oil and gas operations. Some of the many advancements provided by an improvement in downhole sensing is seen in drilling, stimulation, production forecasting, and wellbore integrity. Currently, downhole pressure sensors on the market are costly, cannot be distributed throughout a wellbore, and have a limited lifespan. As a result, a low-cost, all-digital downhole pressure sensor for permanent, distributed installation is being proposed. The planned sensor will measure pressure up to 10,000 psi with a temperature limit of 250°C. The objective for this study was to design the pressure system, validate the sensor under downhole pressure and temperature conditions in a laboratory apparatus, and to prepare a field validation test of the sensor system.

The pressure housing was designed as a cylinder steel tube surrounding the actual sensor while maintaining a limited outer footprint to withstand the required temperature and pressure. Two different end caps were developed. The first cap was developed to allow fluid flow to the sensor system within the housing without damaging the sensor itself. The second cap was designed to allow the sensor's electrical requirements and pressure reading to be transmitted from the surface to the sensor and vice versa without fluid penetrating the housing. The housing pressure and temperature ratings were validated with finite element modeling. Laboratory tests was performed and showed the pressure sensors behaved as expected. A field installation plan was prepared for installing the sensor in a wellbore. The sensor and reference gauge was successfully placed at a depth of 2,550 feet, run the connection lines for the sensor and reference gauge from the placement depth to the surface and connected them to their respective surface acquisition systems, and sealed the wellbore at the surface at 1.5x hydrostatic pressure about 1,300 psi. A workover rig and crew were used to lower the system into the wellbore and install the wellhead, while a hot oiler truck was used to pressure the wellbore through the wellhead design. Three cyclic pressure tests were

conducted, and a drift test of two weeks was successfully done. The field test showed that the sensor was operating within specifications and showed no drift. After the test, we examined the sensors out of the wellbore. There are no signs of leakage; the sensor still functions well.

Chapter 1: Introduction

1.1 Background

The use of downhole pressure sensing has risen significantly in the field of oil and gas operations. One area where downhole sensing technology has proven invaluable is drilling operations. Operators can make informed decisions and optimize the drilling process for improved efficiency and safety by accurately monitoring and measuring pressure conditions deep within the wellbore. Furthermore, downhole pressure sensing plays a crucial role in stimulation activities. It enables operators to precisely assess and control pressure levels during well-stimulation processes such as hydraulic fracturing. This precise monitoring enhances the effectiveness of stimulation techniques, leading to enhanced well productivity and increased recovery of oil and gas reserves.

Historically, operators have experienced less-than-desirable success rates for long-term downhole pressure monitoring, especially in multizone, open-hole, horizontal wells (Marcuccio et al., 2015). One of the major obstacles in developing a lasting and accurate downhole pressure sensor is that current sensors require on-site signal processing, which causes the equipment to be costly due to the large number of sensors needing to be deployed in a production wellbore. Furthermore, the high-temperature electronics and the drift of electrical components in high temperature environments over time raise challenges for permanent sensor installation.

1.2 Types of down hole pressure sensors

Downhole monitoring is challenging. The challenge is caused by the harsh conditions in the subsurface with high temperatures up to 450ºF, and high pressures up to 30,000psi, as well as in the wellbore where strong vibration, and presence of brine, mud, debris, hydrate, and various gases causes sensor failure and poor readings. The long distance of data transmission to the surface causes signal losses. All these challenges have to be overcome to obtain the required reliability and service lifetime of downhole sensors.

A typical electronic sensor includes four functional elements:

1. The transducer (i.e., sensing component).
2. The signal conditioning circuit (e.g., signal conversion, amplification, digitization, etc.) and data telemetry unit.
3. Signal transmission element (e.g., a long cable).
4. Surface electronics (e.g., data recording, presentation, analytics).

There are multiple pressure transducers in the market using electric resistivity, magnetism, piezoelectricity, resonance and optics. For all sensors the working principle is to observe a change in the sensing element with the applied pressure, and this change is measured and converted into an electrical output. For instance, strain gauge pressure transducers using a metal foil or wire strain gauge element which deforms under pressure. Capacitive pressure transducers use a diaphragm that deflects under pressure, changing the capacitance between two plates. Furthermore, piezoelectric pressure transducers employ a piezoelectric material that generates an electrical charge when subjected to mechanical stress and when pressure is applied it deforms. resonant wire pressure transducers consist of a natural frequency resonating wire or tube and the pressure causes a change in the wire's tension or the tube's length, causing a resonant frequency shift. Optical transducers measure pressure-induced changes in the refractive index of the sensing material modulate the intensity, phase, or polarization of light, which is then detected and converted into an electrical output. These are some of the common types of pressure transducers. Each type has its advantages, limitations, and applications, so the choice of transducer depends on factors such as the pressure range, accuracy requirements, environmental conditions, and specific application needs.

The transducer signal is intrinsically weak and analog and cannot be directly transmitted over the long noisy cable. An on-spot circuit must amplify/ condition/digitize the transducer signal to reach the surface. In addition, a close-by data telemetry unit has to be used to relay/transmit the signals to the surface. There are a number of issues with downhole pressure sensors, which are used to measure downhole pressures over the life of a well. Powering the sensors and transferring signals back to the control system are problems for electrical sensors.

Fiber optic sensors, with advantages such as high resolution, small size, and long-distance access, are seen as a suitable candidate for downhole applications (Qi et al., 2002). A fiber optic downhole sensor does not need on-site electronics placed in the downhole environment. The hermetically packaged optical fiber acts as both the distributed sensing element and the signal transmission medium (Bense, et al, 2016). The most popular configuration of fiber optic down-hole sensors involves using various time-domain techniques to realize truly distributed sensing (Holley and Kalia, 2015). Continuous temperature profiles along the entire length of an optical fiber can be mapped with decent accuracy by several mechanisms, including Rayleigh scattering, Raman scattering, and Brillouin scattering (Schenato, 2017; Tardy, et al, 2011; Bateman, et al, 2013; Koelman, et al, 2011; Costello, 2012; Mateeva, et al, 2014; Joe, et al, 2018). These systems are commercially available for distributed temperature, strain, and acoustic measurement in downhole. However, the fiber is sensitive to temperature and stress only; fiber optic pressure measurements rely on discrete optical fiber components such as a packaged interferometer or a Bragg grating such as Halliburton's FiberPoint pressure gauge(Halliburton, 2020). Limitations associated with fiber optic sensors are the sensitivity to temperature and strain as well as the presence of hydrocarbon in the subsurface causing hydrogen darkening in the sensing element.

The installation of permanent downhole pressure sensors is expensive and there are still significant limitations with longevity and robustness of fiber optic pressure sensors and the ability to install distributed pressure sensors. There is a need to develop robust affordable permanent distributed downhole pressure sensors.

1.3 Thesis objectives

This thesis is part of the DOE project DE-FE0031781 titled *"All-digital Sensor System for Distributed Downhole Pressure Monitoring in Unconventional Fields"* which project seeks to develop and validate (through field tests) a new low-cost all-digital pressure sensing technology for in situ distributed downhole pressure monitoring in unconventional oil and gas (UOG) fields. The all-digital sensing technology uses a built-in nonelectric analog-to-digital converter (ADC) to transform the pressure information into a combination of binary (ON/OFF) states. As such, the proposed system does not need downhole electronics for signal conditioning and telemetry. The all-digital sensors can be remotely logged over a long distance, and many sensors can be multiplexed for distributed sensing.

The all-digital sensors eliminate the need for downhole electronics making the new sensors more robust, cost efficient and minimizing drift in comparison to existing sensors. Because the sensor outputs are digital in nature, the new sensors can be remotely logged over long distances, and numerous sensors can be digitally multiplexed for distributed sensing using a single surface interrogation instrument to significantly reduce cost. Through the research and engineering, these technical innovations will result in a new affordable tool that has the ability to enhance the understanding of UOG reservoir behavior, optimize stimulation and production, improve recovery efficiency, and expand the development of emerging UOG plays. In addition to distributed pressures sensing, the all-digital sensing concept could be developed into a new multiparameter sensing platform that includes temperature and acoustic parameters. Coupled with pressure data, the permanently installed all-digital monitoring system will fill critical data gaps in big data analytics and machine learning applications to enhance decision making and improve the ultimate recovery of UOG).

The objective of this thesis is to develop a pressurized chamber and downhole installation methods to deploy the sensor system in a field trial. To meet the objective the thesis project has the following three tasks.

1. Design and manufacture a pressure housing for the sensor system.
2. Validate pressure housing with FEA simulation and laboratory pressure test.
3. Develop and manufacture a deployment system for the sensor to perform a field wellbore test of the complete sensor system.

The design and manufacture for the pressure housing for the sensor system is given in Chapter 2. Chapter 3 presents the results for the FEA verification of the pressure housing and laboratory leakage test. Chapter 4 gives the field verification test plan and installation. Chapter 5 gives the results for the sensor field test.

Chapter 2. Pressure Housing Design

In this section, the design and modeling and manufacturing of the external pressure housing for the developed sensor will be described. The sensor housing consists of three main parts– the tube, the wire cap, and the flow cap. Together, these three parts will protect and allow for proper operation of the sensor in high pressure, high temperature environments. Thus, the pressure housing operating parameters must match the sensor's parameters at a minimum.

2.1 Sensor Housing Design Methodology

Before the design of the pressure housing could begin a list of requirements for the design and verification of the pressure housing system needed to be created to achieve a successful outcome. In order to withstand the challenging conditions of the harsh downhole environment, characterized by elevated temperatures and extreme pressure, we must develop a durable pressure sensor capable of functioning reliably over extended periods. A comprehensive review of existing unconventional oil and gas fields, leading us to determine the required pressure and temperature specifications, was 10,000 psi and 250°C respectively (Na, 2024).

2.1.1 All-Digital Pressure sensor

The all-digital pressure sensor system concept is developed by Clemson University and consists of a downhole sensor, signal transmission cables connecting the sensor to the surface readout box (Xiao and Zhu, 2019). The downhole part of the sensor system is shown in Figure 1. At the bottom of the sensor an open tube to the environment is where the transducer element is exposed to the elevated pressure. The sensor element is made up of a helical Bourdon tube coiled six full rotations. The details of the helical Bourdon tube design and the sensor can be found in Xiao et al. (2024). When pressure is increased inside the tube the helical Bourdon tube will rotate and the upper end of the Bourdon tube is free to rotate while fixed in the vertical directions. The rotation of the Bourdon Tube is for a conventional Bourdon Tube pressure sensors displayed on a dial gauge. However, for this sensor the Bourdon tube is fixed to a vertical rod with conductive contact pins that is sliding across eight digital encoding pads (i.e. digitizer). The digital encoding pads are made up of pattern of conductive and non-conductive material that cause each encoding position to have a unique readout and transferring the rotation into 8 position locations. Each of the digital encoding pads are connected to a wire that can be individually interrogated from the surface giving an eight-bit digital readout of the sensor at the surface. The diameter of the encoder is 60 mm (2.36 in.) and the total length of the sensor including the pressure inlet is 380 mm (22 in.). A 3 mm thick cylinder is encompassing the sensor to hold the parts together. In addition, a hermetically sealed pressure housing is to be designed and placed outside of the sensor to isolate the sensor from the downhole environment.

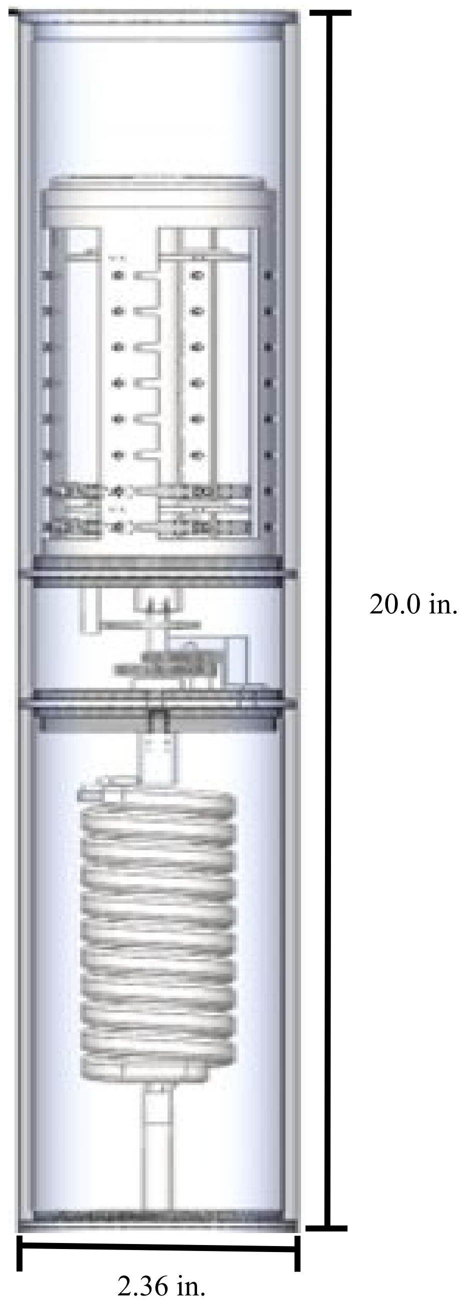

Figure 1. Schematics of the Sensor

2.1.1 Design Objectives of the Pressure Housing System

The following design objectives were established for the pressure housing system.

a. Seal the internal packaging of the sensor.

b. Allow fluid to flow only to coil of internal packaging.

c. Allow sealed electrical cables to exit housing without allowing fluid flow into housing.

d. Maintain working conditions up to 10,000 psi and 482°F (250°C).

e. Availability and cost of materials.

The pressure housing consists of an enclosing tube and two endcaps. On the top there is a wire cap with a pressure seal where the wires are leaving the housing. The bottom endcap has open ports will allow pressure to be transmitted from the outside into the Bourdon

2.1.2 Selection of Pressure Housing Tube

To seal the sensor on **Figure 1**. a cylindrical tube needed to be selected with an inner diameter larger than the outer diameter of the sensor equaling 2.36 inches, the inner diameter of the tube must be equal to or greater than 2.36 inches. A snug fit of the sensor inside the tube was desired to limit the possibility of damage from the sensor moving inside the protective housing. Thus, only an internal diameter range of 2.36 inches to 2.50 inches was considered for the development of the tube housing.

To meet the working conditions up to 10,000 psi and 482°F wall thickness of the material had to be determined. Collapse pressure of the tubing was the only pressure considered because pressure will only be applied externally to the tube during operation. There are four types of collapse pressures: yield strength collapse, plastic collapse, transition collapse, and elastic collapse. Yield strength ($D/t \leq 15$) and elastic collapse ($D/t > 25$) are based on the nominal outside diameter to wall thickness ratio while plastic and transition collapse ratios typically range from 15

< D/t ≤ 25. Equation 1 was used to calculate the collapse pressure for each size of pipe where P_{Yp} is the yield strength collapse pressure, Y_p is the yield strength, D is the nominal outer diameter, and t is the wall thickness.

$$P_{Yp} = 2Y_p[\frac{\left(\frac{D}{t}\right)-1}{(D/t)^2}] \quad (1)$$

Available tubular goods for the housing are given in **Table 1** from McMaster-Carr (2021) and **Table 2** for tubulars in Halliburton (2021). Based on their supply of steel tubes, an internal diameter of 2.50 inches was going to have to be used. Table 1 shows the different options provided by McMaster-Carr® depicting each outer diameter, inner diameter, wall thickness, yield strength, nominal outer diameter to wall thickness ratio, and collapse pressure.

Table 1. Tube Characteristics from McMaster-Carr®

Pipe Type	**Nominal Outer Diameter, in.**	**Inner Diameter, in.**	**Wall thickness, in.**	**Yield Strength, psi**	**D/t**	**Yield Strength Collapse Pressure, psi**
Multipurpose 304 Stainless Steel	3.00	2.50	0.25	30,000	12	4,584
Multipurpose 304 Stainless Steel	3.25	2.50	0.375	30,000	8.67	6,123
Multipurpose 304 Stainless Steel	3.50	2.50	0.50	30,000	7	7,346
Corrosion-Resistant 316 Stainless Steel	3.00	2.50	0.25	30,000	12	4,584
Corrosion-Resistant 316 Stainless Steel	3.50	2.50	0.50	30,000	7	7,346
Easy-to-Weld 4130 Alloy Steel	3.00	2.50	0.25	70,000	12	10,695
Low-Carbon Steel	3.00	2.50	0.25	45,000	12	6,875
Low-Carbon Steel	3.50	2.50	0.50	45,000	7	11,021

The next place considered for material for the design of the tube was using production tubing designed for the oil and gas operations. Using Halliburton's Redbook® (Halliburton, 2021) several options were evaluated.

Table 2. Tubing & Collapse Pressures for 2.875-inch Tubing (Halliburton 2020)

Grade of Pipe	**Weight of Pipe, lbs/ft**	**Inner Diameter, in.**	**Wall Thickness, in.**	**D/t**	**Yield Strength, psi**	**Redbook Collapse Pressure, psi**
F-25	6.40	2.441	0.217	13.25	25,000	3,870
H-40	6.40	2.441	0.217	13.25	40,000	5,580
J-55	6.40	2.441	0.217	13.25	55,000	7,680
LS-65	6.40	2.441	0.217	13.25	65,000	9,070
C-75	6.40	2.441	0.217	13.25	75,000	10,470
L-80	6.40	2.441	0.217	13.25	80,000	11,170
N-80	6.40	2.441	0.217	13.25	80,000	11,160
C-90	6.40	2.441	0.217	13.25	90,000	12,380
T-95	6.40	2.441	0.217	13.25	95,000	12,940
P-105	6.40	2.441	0.217	13.25	105,000	14,010
P-110	6.40	2.441	0.217	13.25	110,000	13,080

2.1.3 Wire Caps for the Field Test

The purpose of the wire cap is to keep the pressure housing sealed while allowing the electrical wires to send the pressure to surface to safely exit the vessel. To prevent any ledges for getting the sensor stuck during installation it was decided to create a seamless design. This meant the outside diameter of the cap would be equal to the outside diameter of the protective tubing

2.1.4 Flow Cap

The core objective of the flow cap is to allow fluid to flow to the appropriate portion of the internal packaging without damaging the electrical components. Supplementary objectives of the design of the flow cap include i) rounded edge to prevent damage while lowering downhole and ii) a hexagonal section on the exterior design to allow a wrench to tighten and loosen the flow cap or strapping of vessel to lower downhole.

2.2 Design Results

2.2.1 Design of the Tube

From Table 1, the D/t ratios can all be seen to be less than 15; thus, making each collapse fall under the yield strength collapse category. Because the room available downhole to place and operate the sensor is critical, the goal is to optimize the outer diameter of the tubing to the smallest diameter possible while maintaining the operational parameters. As a result, tubing with an outside diameter of 3.5 inches or greater was not considered in the design of the pressure housing tube. In future designs, the goal is to reach a maximum outside diameter of 2.00 inches. One can see from Table 1 that only two options have a collapse pressure above 10,000 psi. However, the low-carbon steel option can be eliminated from consideration due to wanting to produce the smallest outer diameter possible leaving the easy-to-weld 4130 alloy steel tube as the option from McMaster-Carr®.

As previously stated, an inner diameter greater than 2.36 inches is needed for the internal packaging of the sensor to fit. When it comes to oil and gas casing and tubing, sizing is described in the nominal outer diameter. Because through McMaster-Carr®, an outer diameter tube dimensions of 3.00 inches could be used, only outer diameters of less than 3.00 inches were considered from the oil and gas piping. The next two nominal sizes smaller than 3.00 inches are

2.875-inch and 2.375-inch pipe. However, because these are outer diameter sizes, 2.375-inch pipe cannot be considered. Because only 2.875-inch pipe will be considered, Table 2 is understood to have a nominal pipe size of 2.875 inches while providing the grade of pipe, weight of the pipe, inner diameter, wall thickness, D/t ratio, yield strength, and collapse pressure. The Redbook® provides the collapse pressure to the nearest 10 psi.

Unlike McMaster-Carr® the Redbook® has all similar dimensions, so the choice was made strictly from the collapse pressure and price. While price is not listed, price typically increases with increase in grade. One can see from Table 2 that any grade of pipe above C-75 meets the collapse parameters needed to operate the sensor. However, after research into local supply and to an additional safety margin on the collapse pressure, it was decided the N-80 grade was the first choice of material. Another decrease in outer diameter can be seen by comparing the N-80 pipe to the easy-to-weld 4130 alloy steel tube (3.00 inches to 2.875 inches). Thus, an overall decision was made to use the N-80 pipe as the material for the tube. Because of the snug fit with an inner diameter of 2.441 inches, less modifications will need to be made during the machining process.

Now that the inner and outer dimensions of the tube have been decided, the total length needed to be determined. One can see from Figure 1 the overall length of the internal packaging of the sensor is 20 inches. To create a sealed external housing without modifying exposed edges of the tube, female threading needs to be added to each end of the tube. Because of the high pressure, high temperature systems the housing and sensor will face, bigger threads were designed for the housing using SolidWorks®. Each threading will have a total height of 1.50 inches. Thus, a total of 3 inches will be added to the length of 20 inches for a total length of 23 inches for the protection tube (**Figure 2**). The threading will cut into the tube in a triangular fashion for a total length of 0.06 inches from the center of the triangle horizontally to the apex of the triangle with a pitch of 0.15 inches giving the threading a total of 10 revolutions from top to bottom (Figure 2). The finished protection tubing due to the known collapse pressure of 11,160 psi from the Redbook® and the specific unknown characteristics of the N-80 grade pipe to conduct an accurate finite-element model.

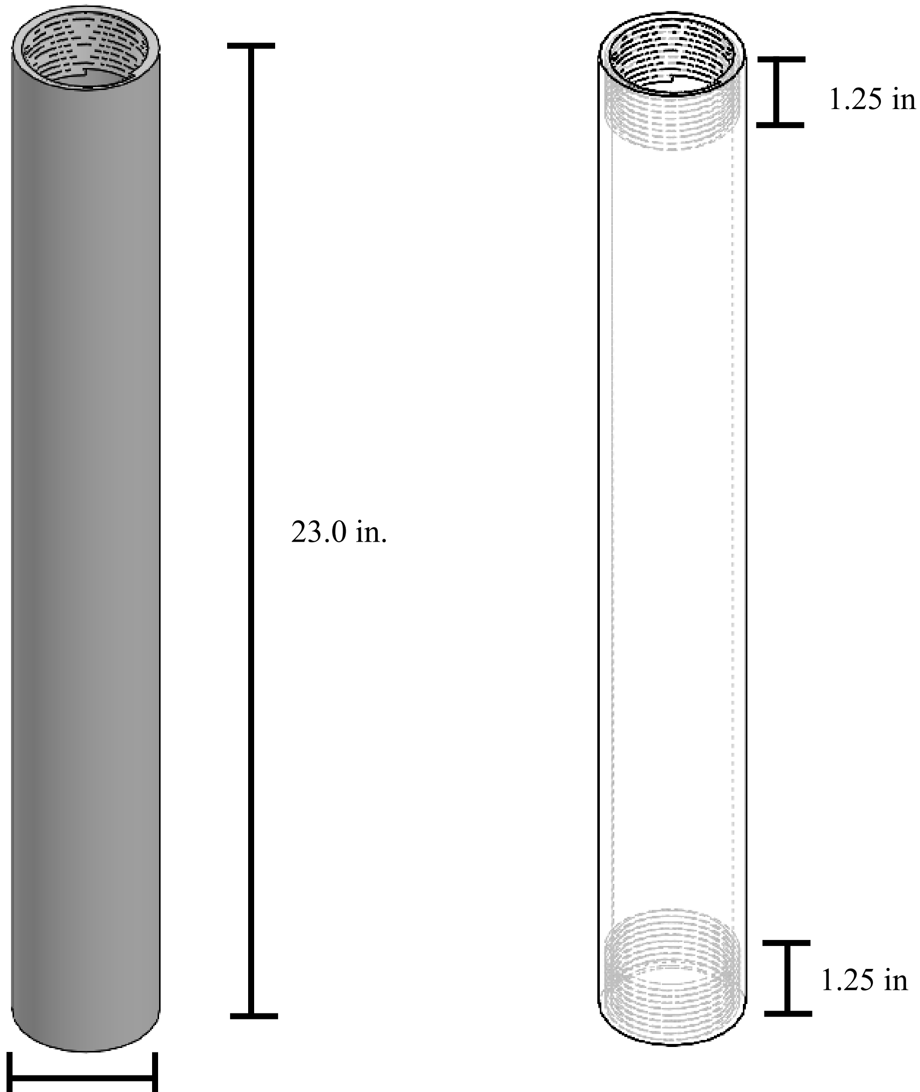

Figure 2. Design of the Protection Tube

2.2.3 Design of the Wire Cap for the Field Test

For ease of screwing and unscrewing the cap, a cylindrical portion of the cap will extend 1.50 inches from the end of the protection tube (fully screwed) to the top of the wire cap. Next, an O-ring groove was designed to ensure sealing of the cap. After the external part of the cap was designed, the male threading was added to the cap. Originally, the male threading was designed to match the female threading of the tube. This design meant from outside to outside of threading, the diameter would be 2.561 inches. 0.12 inches must be added to the inside diameter of the protective tube to account for the female threading cut into its walls (0.06 inches for each side). The depth of the threading matches the depth of the threading on the tube at 0.06 inches in a triangular fashion from the center of the triangle to the apex. The height of the threading was 1.50 inches and a pitch of 0.15 inches for a total of 10 revolutions. An O-ring groove was included to ensure proper sealing of the cap. Thus, a height of 0.25 inches of threading was removed from the design where the threading intersected the larger diameter of the cap. In addition, because this 0.25 inches needs to fit inside the protection tubing, the outside diameter would be equal to 2.441 inches. In the center of the 0.25 inches, an O-ring groove was designed using half of a circle with a diameter, or cross section, of 0.103 inches. **Figure 3** shows the design of the wire cap for the laboratory tests. With the O-ring groove being smaller than the threading, the cap should seal nicely into the protection tubing.

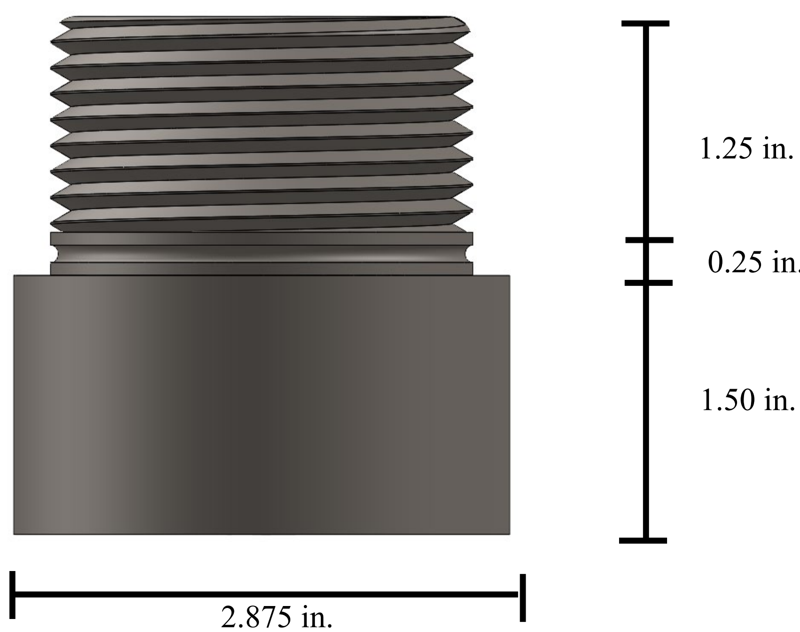

Figure 3. Front View of the Laboratory Wire Cap

The last attribute of the wire cap designed needed before deciding the type of material is drilling the smooth bore hole through the center to allow the cable to travel snuggly through the cap from the sensor to outside the pressure housing. As discussed, a cable containing seven conductors is needed for operation of the sensor in the field test operations. Further discussed there, the cable preliminarily found to work has an outer diameter of 0.37 inches. Thus, the hole designed in the wire cap has a diameter of 0.40 inches as seen in **Figure 4**. This will allow the user to pull the cable through the smooth bored hole with a snug fit sealing the cap.

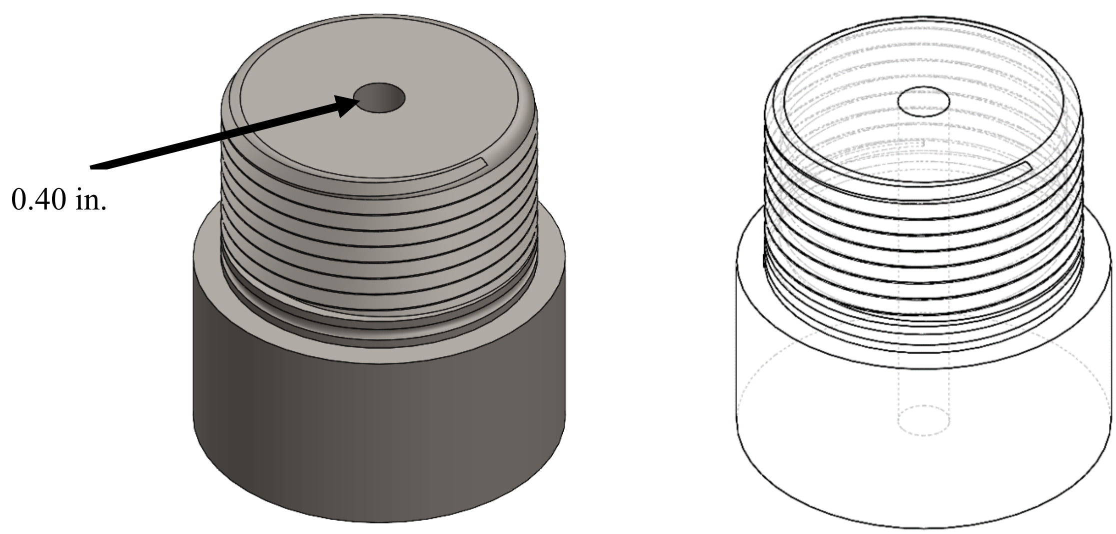

Figure 4. Isometric Views of the Wire Cap for the Laboratory

To finish the design of the wire cap, a material had to to be selected that will hold up in working conditions up to 10,000 psi. First, using McMaster-Carr® all 2.875-inch steel rods possible for use were determined and listed with their yield strengths in Table 3. To determine the collapse pressure of the rods, the type of collapse that would occur needed to be established through the D/t ratio. D is the nominal outside diameter in inches while t is the wall thickness of the material. To determine t, the inner diameter, or size of the wire hole, was subtracted from D. The results are shown in **Table 3**, and one can see the D/t ratio is 1.162 which is significantly less than 15. Because it is less than 15, the type of collapse that would occur would be yield strength collapse. As a result, Equation 1 can be used again to determine the yield strength collapse pressure. As shown in Table 3, there are 4 different materials that meet the collapse pressure requirement of 10,000 psi.

Table 3. 2.875-inch Rods from McMaster-Carr®

Material	**Yield Strength, psi**	**Nominal Outside Diameter, in.**	**Inner Diameter, in.**	**Wall Thickness, in.**	**D/t**	**Yield Strength Collapse Pressure, psi**
Tight-Tolerance Ultra Machinable 12L14 Carbon Steel	65,000	2.875	0.4	2.475	1.162	15,597
Ultra-Machinable 12L14 Carbon Steel	60,000	2.875	0.4	2.475	1.162	14,397
High-Strength 1045 Carbon Steel	77,000	2.875	0.4	2.475	1.162	18,477
Multipurpose 4140 Alloy Steel	60,000	2.875	0.4	2.475	1.162	14,397
Multipurpose 304 Stainless Steel	30,000	2.875	0.4	2.475	1.162	7,199
Easy-to-Machine 303 Stainless Steel	25,000	2.875	0.4	2.475	1.162	5,999
Corrosion-Resistant 316 Stainless Steel	30,000	2.875	0.4	2.475	1.162	7,199
High-Strength 630 Stainless Steel	Not Rated	2.875	0.4	2.475	1.162	Undetermined

The next selection criterion for material was determining which of the four materials can withstand temperatures reaching up to 482°F. **Table 4** was developed from a combination of Table 3 and the *ASM Specialty Handbook – Heat-Resistant Materials (Davis, 1997).* From McMaster-

Carr, it was determined the multipurpose 4140 alloy steel is also known as chromium-molybdenum steel (Steel rods, 2023). It can be seen that each of the 4 materials that meet the pressure requirement also meet the maximum temperature requirement. **Figure 5** also shows the effect of tensile strength as temperature increase for various metals and alloys. It can be depicted that molybdenum has an initial decline in tensile strength as temperature increases but flattens around 300°F and 100 ksi until it reaches about 900°F and begins to dramatically lose strength again. On the other hand, carbon steel has an initial rise in tensile strength until it reaches about 475°F and 75 ksi where it begins to decrease in strength slowly until rapidly decreasing around 800°F. Because each of these 4 materials meet the temperature requirements, the decision on which material to use comes down to a final evaluation of cost and availability. As a result, the high-strength 1045 carbon steel rod was selected.

Table 4 - ASM Handbook Maximum Temperatures (Davis, 1997)

Material	**Maximum Working Temperature**
Tight-Tolerance Ultra Machinable 12L14 Carbon Steel	800°F
Ultra-Machinable 12L14 Carbon Steel	800°F
High-Strength 1045 Carbon Steel	800°F
Multipurpose 4140 Alloy Steel	950°F

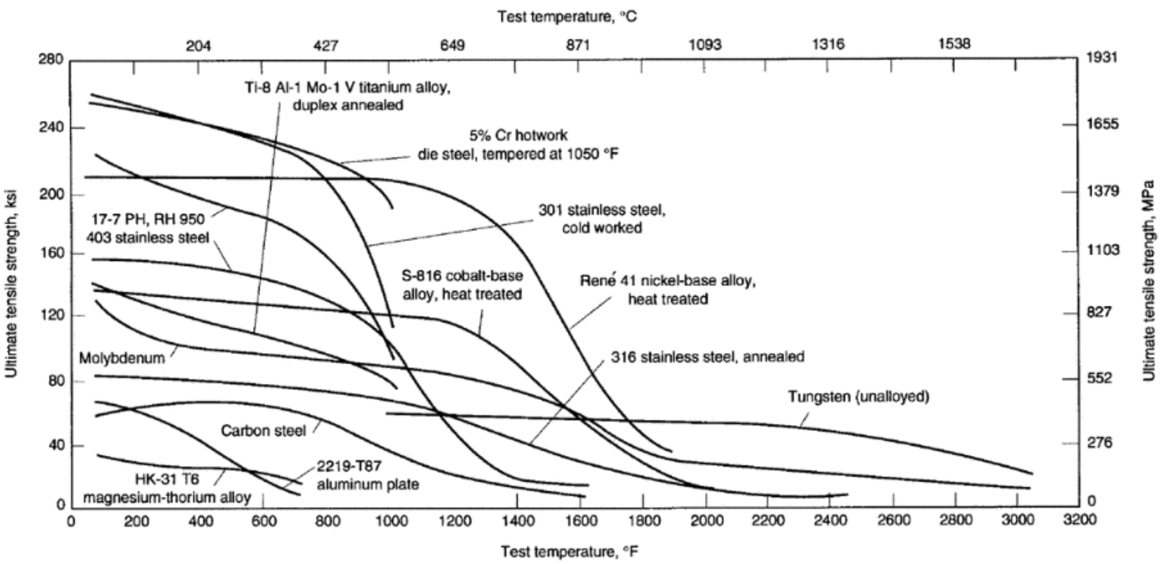

Figure 5. ASM Handbook Temperature vs Ultimate Tensile Strength (Davis, 1997)

2.2.4 Design of the Flow Cap

As discussed in the Design of the Tube and Design of the Wire Cap, threading and an O-ring groove matching the design of the wire cap to fit the tube were created as the starting point for the flow cap. As a review the design meant from outside to outside of threading, the diameter would be 2.561 inches. 0.12 inches must be added to the inside diameter of the protective tube to account for the female threading cut into its walls (0.06 inches for each side). The depth of the threading matches the depth of the threading on the tube at 0.06 inches in a triangular fashion from the center of the triangle to the apex. The height of the threading was 1.50 inches and a pitch of 0.15 inches for a total of 10 revolutions. After further discussion, though, it was deemed an O-ring groove needed to be included to ensure proper sealing of the cap. Thus, a height of 0.25 inches of threading was removed from the design where the threading intersected the larger diameter of the cap. In addition, because this 0.25 inches needed to fit inside the protection tubing, the outside diameter would be equal to 2.441 inches. In the center of the 0.25 inches, an O-ring groove was designed using half of a circle with a diameter, or cross section, of 0.103 inches. Figures 6 and 7 shows the design of the flow cap. With the O-ring groove being smaller than the threading, the cap should seal nicely into the protection tubing. The design of the threading can be seen back in Figure 3.

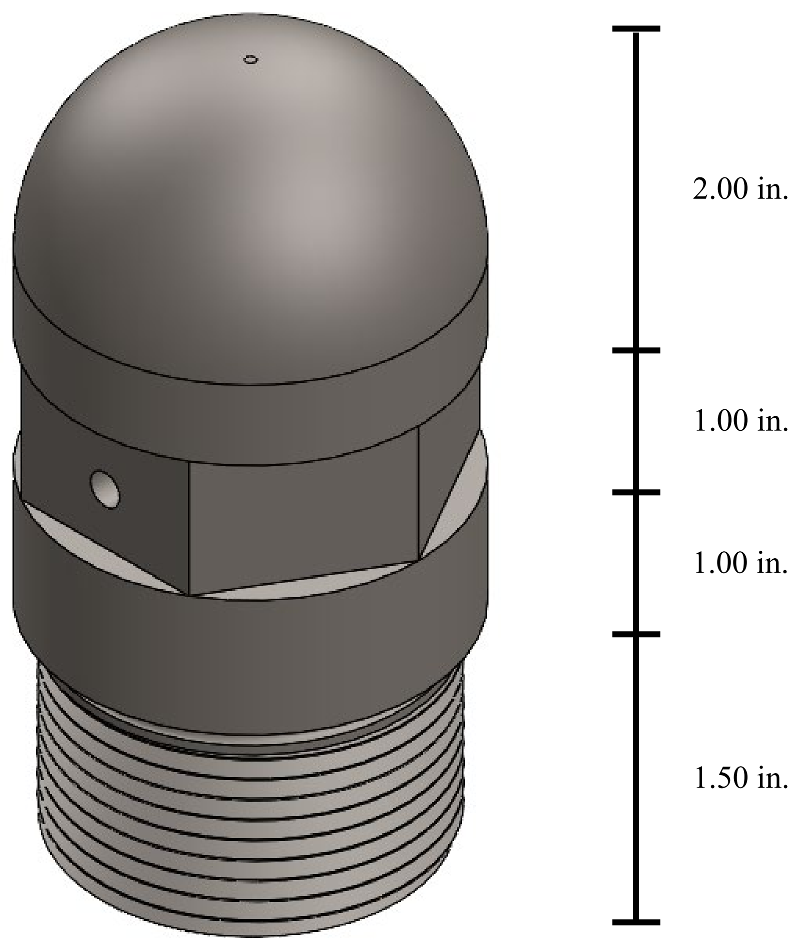

Figure 6. Iso View of the Flow Cap

As seen in **Figure 6** and similar to the wire cap, a lip was created to seal the cap with the exterior of the flow cap designed to sit flush with the exterior of the protective tubing. 1.00 inches of material was created for easy handling of the flow cap between the threading and flow inlets.

Next, as depicted in Figure 6, a hexagonal section with a height of 1.00 inches was created. The hexagonal section completed the design objective and preference for easy handling while tightening or losing the cap and allowing the vessel to be securely strapped to the sucker rods for the field test. The top section of the flow cap has a height of 2.00 inches. This allowed for ample room to fillet the head of the cap into a rounded edge. By having a rounded edge, the vessel will not catch on tubing or formation as the head of the flow cap will be the first edge lowered downhole. The final and core objective to complete is designing a path for fluid to flow into the cap to the coil without spreading elsewhere into the housing. **Figure 7** shows a transparent view of the flow cap design where one can see the fluid path holes. A hole 0.25 inches in diameter was drilled straight through the cap in the middle of a hexagonal cut side. This allows fluid to flow into the cap from either side of the cap. The hole being 0.25 inches in diameter was determined to be suitable for fluid flow without debris entering and clogging the hole. Next, from the bottom of the cap, a hole initially 0.25 inches to match the other hole was drilled for fluid to flow in a controlled manner into the vessel. Using this 0.25 inch hole as a guide, female threading 1.00 inch in length was machined into place. The threading was machined to match 7/16 – 20 NF threads. The 7/16 – 20 NF threading comes from the male threading on the end of the coil of the internal packaging to create a fluid tight environment at the connection point.

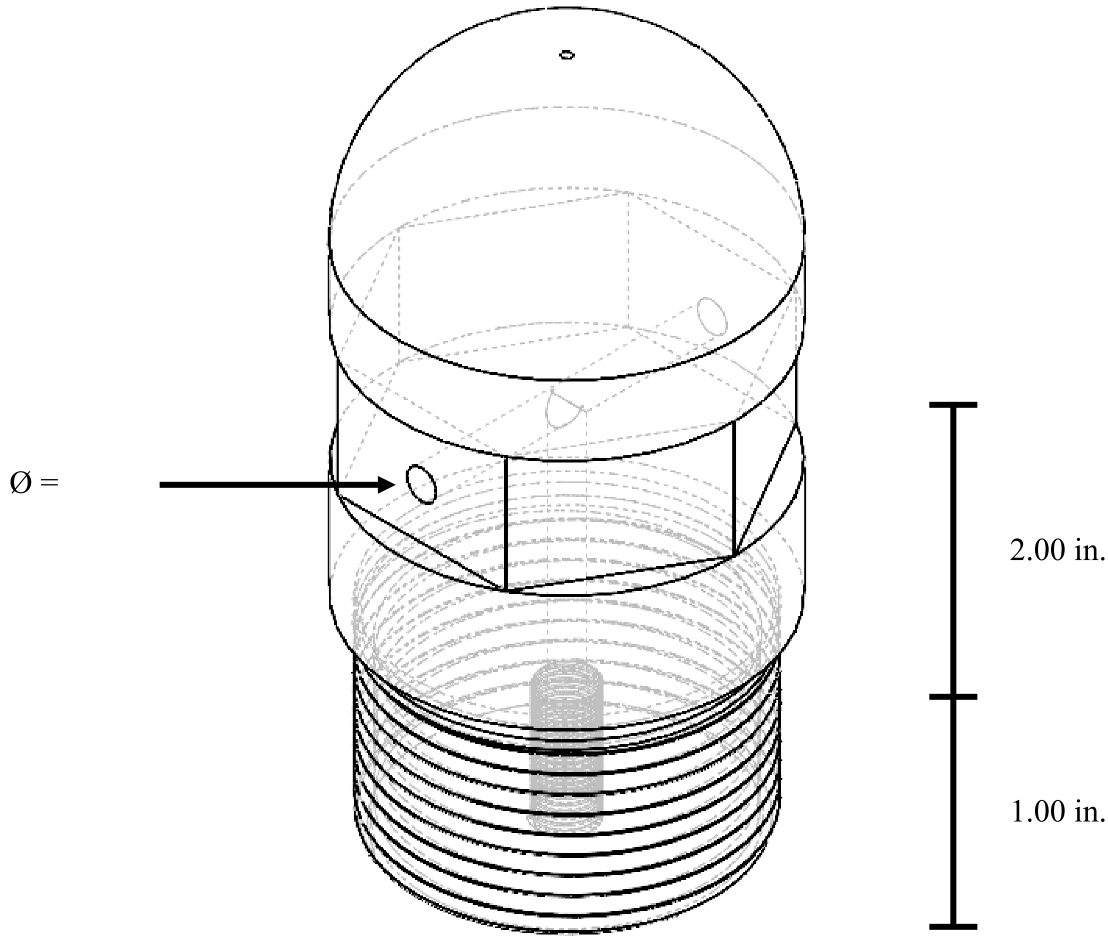

Figure 7. Iso and Transparent View of Flow Cap

2.3 Finite element design verification

To verify the pressure and temperature requirements for the pressure housing design finite element analysis on the individual parts and the fully manufactured assembly was conducted. The methodology and results of the finite element analysis are presented in this section.

2.3.1 Finite Element Methodology

The distinct parts were designed using SOLIDWORKS and presented with detailed illustrations in the previous sections. Subsequently, the finite element analysis was executed in ANSYS 2023. To integrate the SOLIDWORKS drawings into the ANSYS software, the files were saved in the form of STEP files and uploaded. Figure 8 demonstrates the FEA model setup of the pressure housing tube. The tube was discretized into 9723 10-noded tetrahedrons, utilizing linear elastic elements (SOLID187), with a total node count of 20,157 nodes. Fixed supports were applied on both ends of the tube (**Figure 8 a**) and a uniform, 10,000 psi pressure was imposed on the outside surface (**Figure 8 b**).

Equation 2 was used to calculate the burst pressure as a benchmark to evaluate the FEA model. By comparing the simulation results with the "Redbook data" for burst pressure, the accuracy of the FEA can be assessed (Halliburton 2023).

$$P_{burst} = \frac{2 \times T \times S}{D} \tag{2}$$

Where P_{burst} is the burst pressure in psi, T is the wall thickness of the pipe inches, S is the allowable stress psi, and D is the outside diameter in inches.

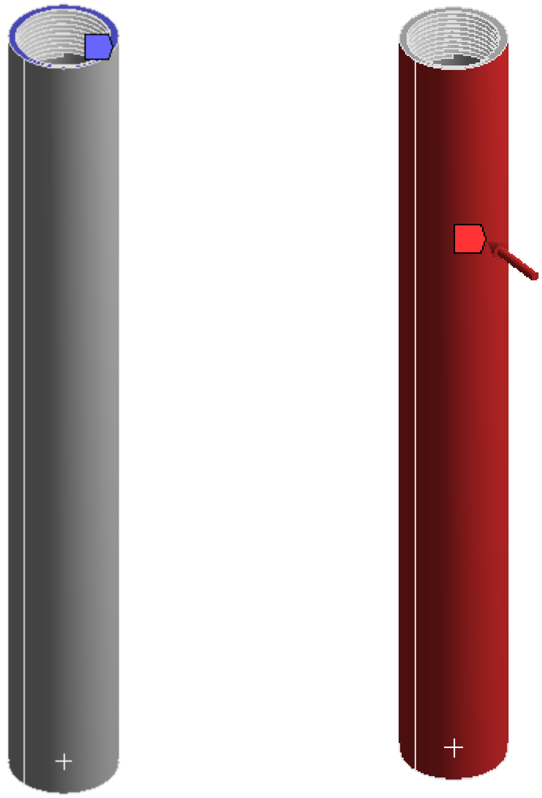

(a) (b)

Figure 8. (a) Fixed support, (b) pressure put on the tube

Figure 9 represents the FEA model design of the pressure housing wire cap. The tube was discretized into 179,536 10-noded tetrahedrons, utilizing linear elastic elements (SOLID187), with a total node count of 607,346 nodes. A fixed support was placed on the end edge (Figure 9 a) and a uniform, 10,000-psi pressure was imposed on the outside surface (Figure 9 b).

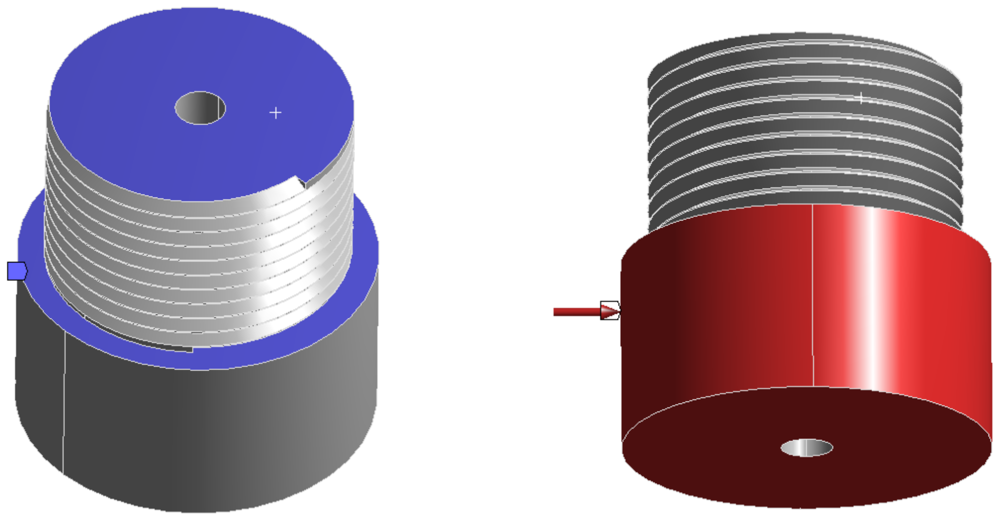

(a) (b)

Figure 9. (a)Fixed support on two surfaces, (b) pressure put on the cap outside

Similarly, **Figure 10** shows the FEA model set up of the pressure housing flow cap. The tube was discretized into 55,390 10-noded tetrahedrons, using linear elastic elements (SOLID187), with a total node count of 159,911 nodes. A fixed support was placed on the end edge (Figure 9 a) while a uniform, 10,000 psi pressure was imposed on the outside surface and the flow passageway in the cap (Figure 9 b).

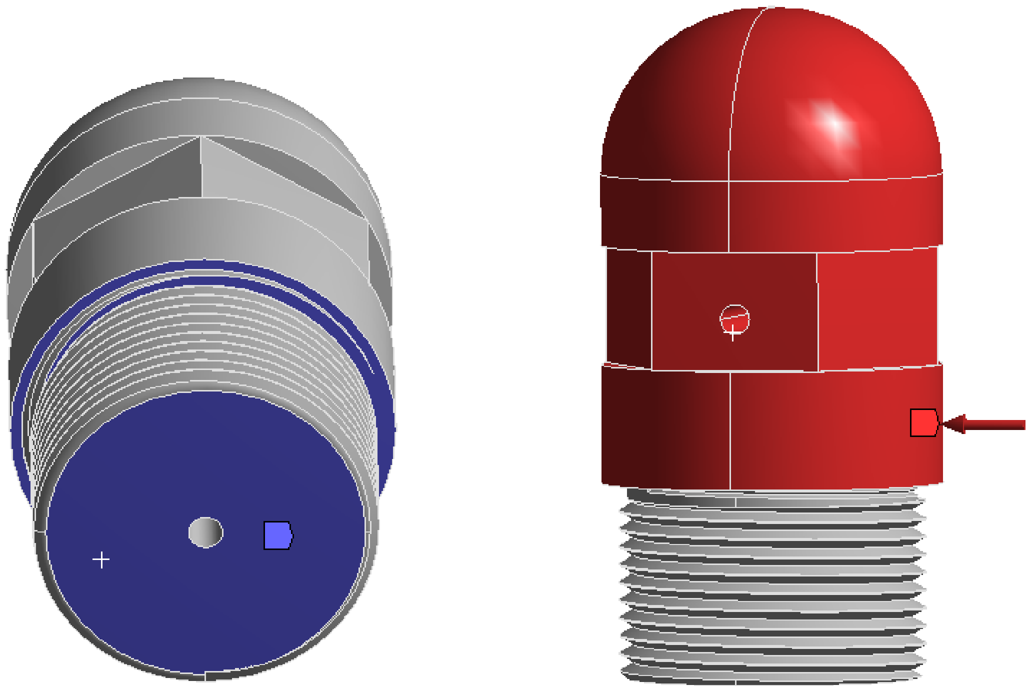

(a) (b)

Figure 10. (a)Fixed support on two surfaces, (b) pressure put on the cap

2.3.2 Finite Element Design Verification Results

Total deformation and equivalent stress tests were performed on the FEA models presented in the previous section. It took ANSYS a total of 3 minutes to perform each simulation run. **Figure 11** depicts the total deformation test result for the pressure housing tube. It has the maximum total deformation of 0.004 inches. The maximum deformation outcome was within the self-imposed standard of 0.005 inches deeming it a successful analysis. **Figure 12** represents the equivalent stress test result for the pressure housing tube. It has a maximum equivalent stress of 82,374 psi. Based on the burst pressure calculation mentioned in section 2.3.1, N-80 pipe has a burst pressure of 12,076 psi. The ANSYS generated model calculated a burst pressure of 12,402 psi. The percentage difference in pressure results is roughly 2.7%. A difference below 3% is an acceptable result (Wise, 2021).

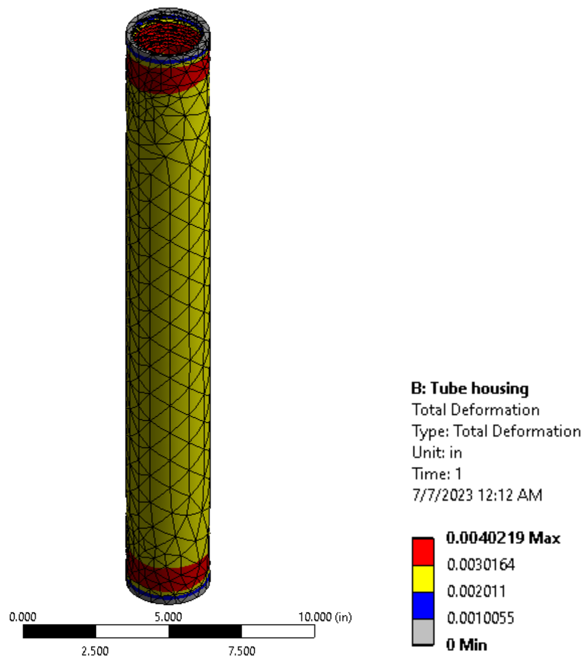

Figure 11. Housing tube deformation

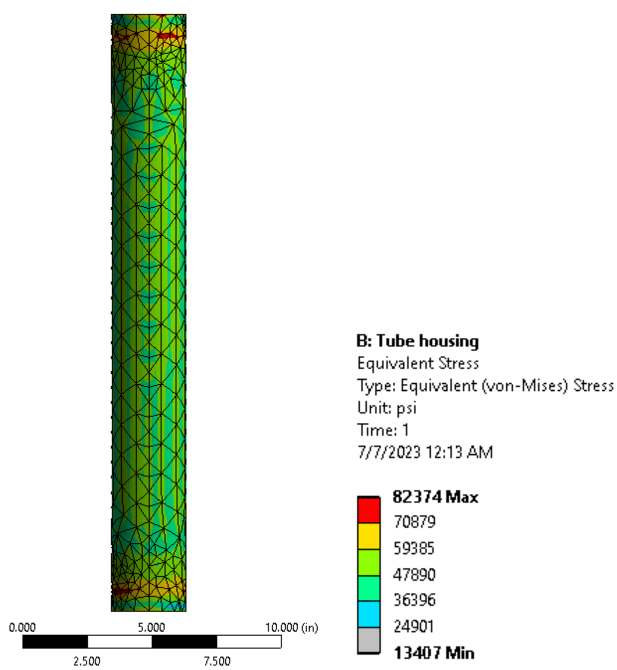

Figure 12. Housing tube stress modeling result

Figure 13 shows the total deformation test result for the pressure housing wire cap. It has a maximum deformation of 0.0005 inches. The maximum deformation result was within the self-imposed standard of 0.005 inches resulting in a successful examination. **Figure 14 (a) & (b)** illustrate the equivalent stress test result for the pressure housing wire cap. It has a maximum equivalent stress of 19,099 psi. Because the equivalent stress result of 19,099 psi is a fraction of the material's yield point of 77,000 psi, this test was considered successful.

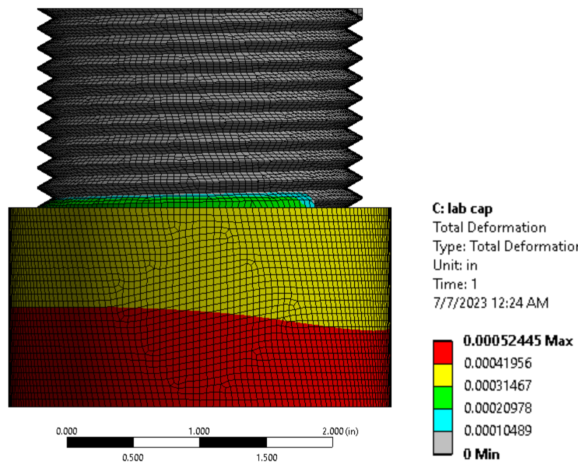

Figure 13. Wire cap total deformation

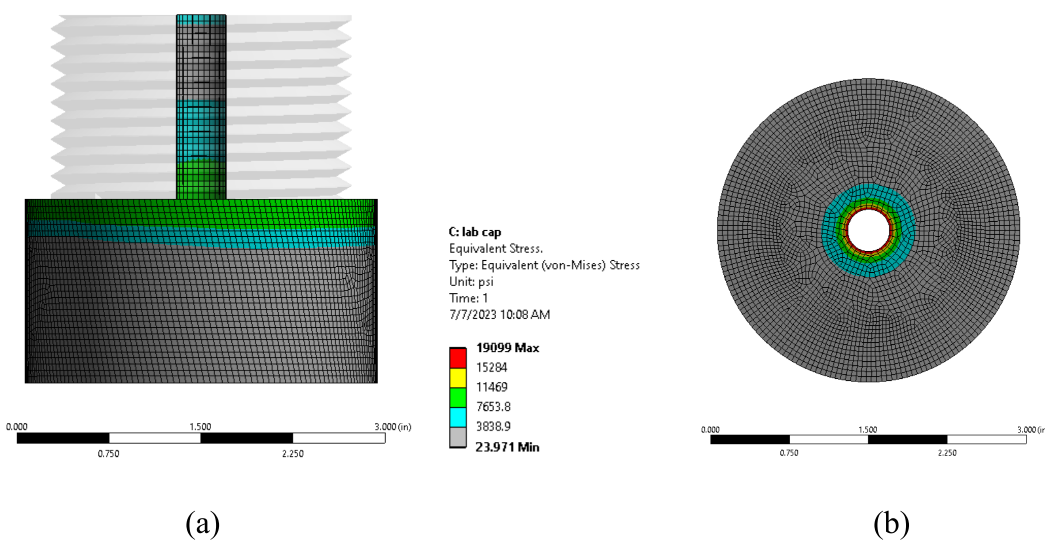

Figure 14. (a) Wire cap stress result, (b) bottom view of the cap

Figure 15 represents the total deformation test result for the pressure housing flow cap. It has a maximum deformation of 0.0016 inches. The maximum deformation result was within the self-imposed standard of 0.005 inches; thus, the test was accepted as true. **Figure 16** demonstrates the equivalent stress test result for the pressure housing flow cap. It has a maximum equivalent stress of 25,355 psi. Similar to the wire cap, the equivalent stress result is a fraction of the material's yield point of 77,000 psi and viewed successful.

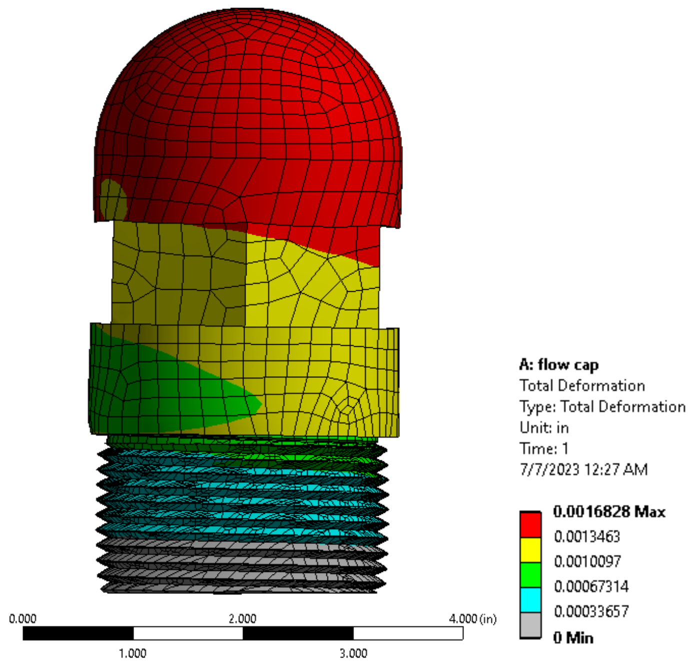

Figure 14. Flow cap total deformation

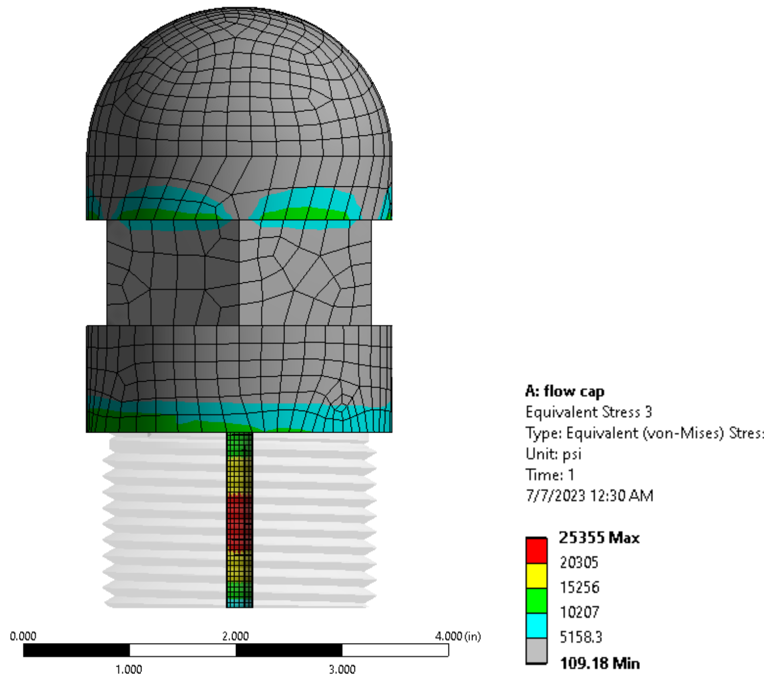

Figure 15. Flow cap stress modeling result

2.3.3 Assembled Housing Verification

After each distinct part was modeled and verified, the assembled housing needed to have an FEA model and stress test performed. **Figure 17 (a)** shows the assembled pressure housing. Similar to the individualized tests, 10,000 psi was placed on the outside of the assembled housing. **Figure 17 (b)** depicts the equivalent stress test results for the assembled pressure housing. It has a maximum equivalent stress of 81,331 psi. This outcome equates to a burst pressure of 12,277 psi. Comparing the model's burst pressure with the burst pressure of the N-80 pipe, there is a pressure difference of 1.6%. This proves an accurate FEA result. In addition, the full pressure housing assembly modeling results match the individual parts conclusions further confirming the findings.

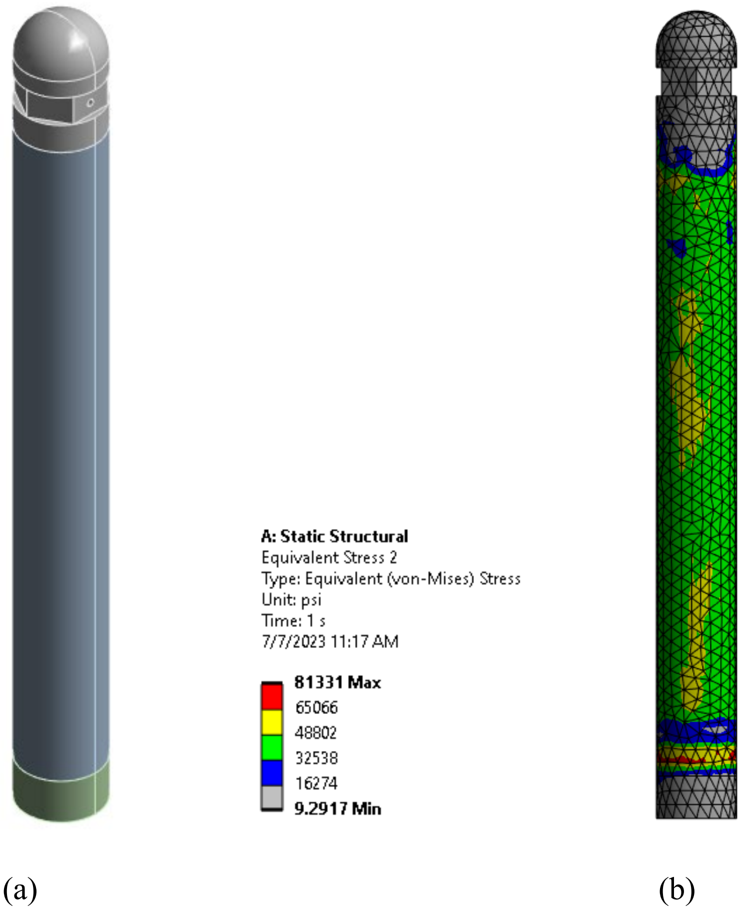

Figure 16. (a) Assembled housing FEA model, (b) Stress result

Chapter 3. Sensor Verification Results

3.1 Experimental setup

The pressure housing design was fabricated for laboratory testing. **Figure 18** shows the fully assembled pressure housing for the sensor's laboratory testing. From the picture, the assembly will be flipped 180 degrees once placed inside the pressure chamber. The fabricated tube is shown in **Figure 19**. The flow cap is shown in **Figure 20**. The Swagelok threading located in the bottom of the flow cap discussed in Section 2.2.4 is shown in **Figure 21 (a)**. In order to perform a laboratory pressure test on the external pressure housing, a replacement cap was produced. The replacement cap replaces the flow cap to create a completely sealed pressure housing. The replacement cap is shown in **Figure 21 (b)**.

Figure 17. Fully assembled laboratory pressure housing.

Figure 18. The fabricated tube of the housing.

Figure 19. The fabricated flow cap of the housing.

Figure 20. (a) Bottom view of flow cap with Swagelok threading (b) Replacement cap without openings.

Figure 21. (a) Sensor assembled to the refurbished replacement cap. (b) Housing and the lid of the chamber.

Due to the constraints of the testing chamber, the replacement cap subsequently had the required Swagelok threading and flow hole added to it. The pressure inlet of the all-digital sensor was connected to the refurbished replacement cap in **Figure 22 (a)**. **Figure 22 (b)** shows the pressure housing tube along with the manufactured lid of the testing chamber. The manufactured lid was necessary to secure the pressure housing inside the testing chamber and still allow the necessary wire requirements to extrude from the sensor to the data acquisition system. Next, the sensor was placed in the pressure housing tube and secured with the refurbished replacement cap & lid of the testing chamber. **Figure 23** shows test assembly prior to the refurbished replacement cap being screwed into the pressure housing tube. The test chamber was pre-filled with water before placing the pressure housing and sensor assembly into it. Lastly, a Teledyne-ISCO 100DX syringe pump was connected to the testing chamber capable of generating pressures of up to 10,000 psi. The pump was connected to the chamber through a 1/8-inch inner diameter tubing with two pressure valves from Swagelok. The test setup is shown in **Figure 24**.

.

Figure 23. All-digital sensor assembled with housing and testing chamber lid

Figure 224. Test setup

Due to design constraints of the sensor itself, the Teledyne-ISCO 100DX syringe pump was only used to generate pressures up to 2,000 psi. Heating tape and insulation were wrapped around the outside of the testing chamber to control the required testing temperatures. A DAQ was used to read the sensor. A thermal coupler was used to monitor the inner temperature of the testing chamber. The sensor was tested at 23 ℃, 50 ℃, and 73 ℃, respectively. Using an incremental/decremental step pattern of about 100 psi, the pressure of the testing chamber was increased from 0 psi to 2,000 psi and back down for each required temperature.

3.2 Results

The pressure responses were similar for all three testing temperatures. The sensor showed to have a linear response in the range of 0 to 2,000 psi. The sensor had about 100 psi hysteresis (difference between pressure-increase and pressure-decrease response lines). One explanation of this result could be explained by the friction force between the contact pins and encoding pads in the sensor itself. A possible solution is to replace the contact pins with small bearings, thereby mitigating the frictional forces during their movement on the encoding pad. The results of the temperature-pressure test are found in **Figure 25**.

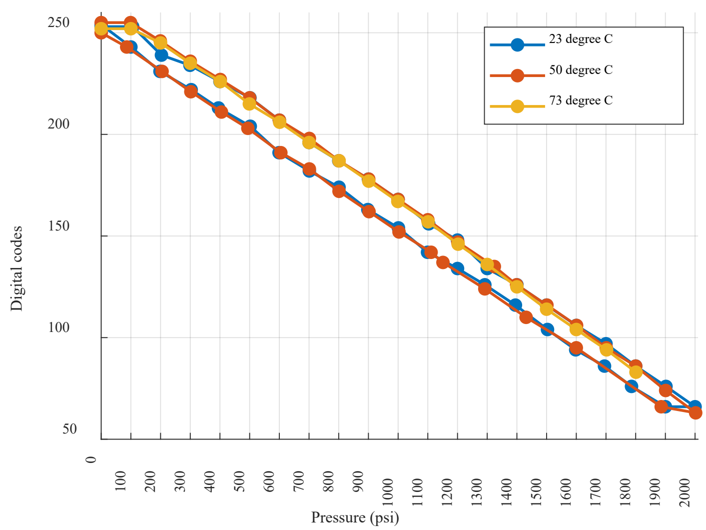

Figure 23. Laboratory pressure testing results at different temperatures

Chapter 4. Field-Testing Plan

4.1 Overview

The following chapter outlines the development of the field-testing procedure for the newly designed sensor. Two major areas of concern were identified when creating the test plan. These areas included i) the wellhead system and ii) how the sensor would be lowered into the wellbore. A set of criteria is outlined later in the chapter that each area must satisfy to have a successful operation of the sensor. After the design of the testing features needed to perform the test was completed, the testing conducted on the sensor was defined.

4.2 Well Location

The field test will be conducted at Quest Testing Facility located at 101 W 80th Street, Stillwater, Oklahoma 74074. The Quest Testing Facility is located on 118-acres and lies west of U.S. Highway 177 on West 80th St., 5 miles south of Stillwater, Oklahoma. This facility currently has 5 test wells on site with available drilling and production equipment. The location of the field test site is shown in Figure 1. The Quest Testing Facility team is led by Brian McCutchen and will be working in conjunction with the OU testing team led by Dr. Runar Nygaard.

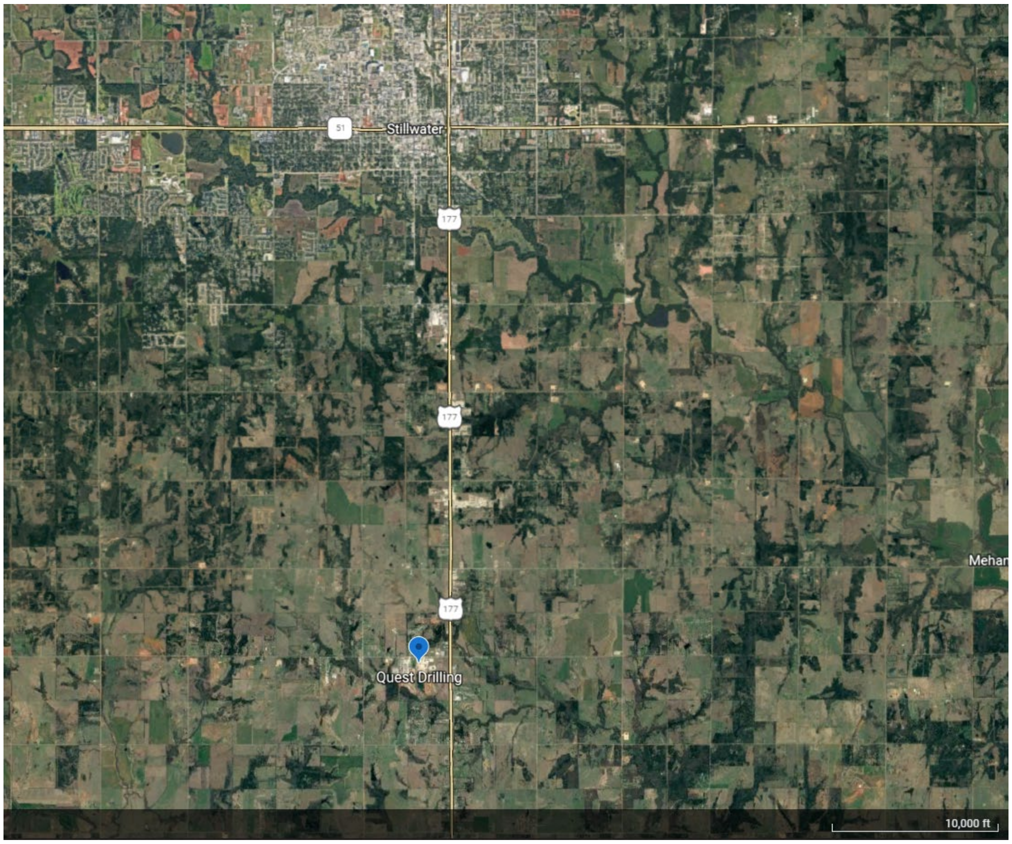

Figure 24. Location of Quest Drilling Facility

4.3 Procedure

4.3.1 Wellbore Preparation

The team will be using 1 of the 5 test wells at the Quest Drilling Facility for the project. The well selected for use in this project (shown in **Figure 26**) was drilled and completed to an original depth of 5,000 feet; however, testing will be conducted at a depth of 3,000 feet. The hole is currently plugged with a cement barrier plug. The Quest team will drill out the plug and swab the hole to a depth of 5,000 feet to ensure the hole is clear of any debris that may interfere with the testing of the sensor downhole. The hole is cased with 7-inch production casing to the full depth of 5,000 feet and will not be changed. An existing 11 5/8-inch casing head is attached to the top of the wellbore at ground level to allow for any wellhead connections to be connected. Once the Quest team is finished cleaning the hole, they will remove the drilling equipment and clear the hole at the surface for further project operation.

4.3.2 Getting the Cables to the Surface and Wellhead Design

Current design of the sensor requires 9 conductors be ran to the surface for its operation. This number of conductors creates a challenge in getting them all to the surface. Regular cables, wellheads and hanger systems used within the petroleum industry are designed for a 3-wire system. The 7/32” mono-conductor cable described in the previous section has only 1 conductor inside of it. To run the all-digital-sensor and reference gauge to their full 10,000 psi range, a total number of 10 conductors are needed. However, due to the controlled pressure environment of the field test, the total number of conductors needing to be run to the surface for the project is eight conductors. Eight conductors are significantly higher than the industry standard of three or less. After understanding the total number of conductors needed to perform the test, a complete set of criteria was developed that the wellhead system must meet in order to perform the field assessment.

The Wellhead System Criteria

a) Handle eight conductors passing from the wellbore to the surface.

b) Seal around the conductors to avoid leakage and maintain constant wellhead pressure.

c) A minimum surface pressure of 1,500 psi.

d) Ability to circulate up to 100°C fluid for heated temperature test.

**If multiple wellhead systems meet all criteria listed above, then those systems will be evaluated on the availability and economics for best fit. **

Three wellhead systems, i) a fit-for-purpose designed system, ii) a dual completion head system, and iii) a casing spool and annular BOP system, were proposed and evaluated on the criteria listed.

First, a wellhead and hanger system were designed by TechnipFMC to handle the large number of conductors needed to be run the testing. The design can be found in Appendix A. A preliminary decision was also made to run multiple electronic submersible pump (ESP's) cables (each cable contains 3 conductors) to meet the sensor demands for the field test. As a result, a triple hanger design was developed as each hanger would allow for 3-4 conductors to pass through the wellhead while keeping the wellbore sealed. The wellhead itself is a 3k system meaning it can handle a surface pressure up to 3,000 psi. A 5k system was also discussed, but it was deemed too expensive as the 3k system would suffice. The wellhead would be seal on the top as this well is not a producing well. Two flanges were included into the design to allow for fluid circulation to create pressurization and temperature variance within the wellbore.

The next solution to get the wires out of the wellbore uses a dual completion head **(Figure 27**). As mentioned, a 11.625-inch casing head is already installed connecting to the 7-inch casing. Originally, the 11.625-inch casing head would have been replaced with a 9.625-inch collar. In order to get from 9.625 inches to 7 inches, a 9.625-inch by 7-inch swage was to be placed at connecting the collar to the 7-inch by 2.875-inch dual completion head. 2.875-inch production tubing containing the sensor will be attached to one side of the dual completion head (Point E). On the other side of the dual completion head (Point F), a 5-to-10-foot piece of 2.875-inch production tubing will be attached. Instead of strapping the cables to the last joint, or first joint in the hole from the surface, they will be loose and ran through the smaller piece of production tubing to the surface (Point F to Point B). A 2.875-inch pack-off and 3k wellhead would be used to seal the hole and prevent pressure loss all while allowing the cables to exit the well (Point B). The dual completion head is designed with multiple flanges which would allow for fluid circulation to create pressure and temperature variances in the wellbore and the attachment of a pressure gauge to monitor surface pressures during testing.

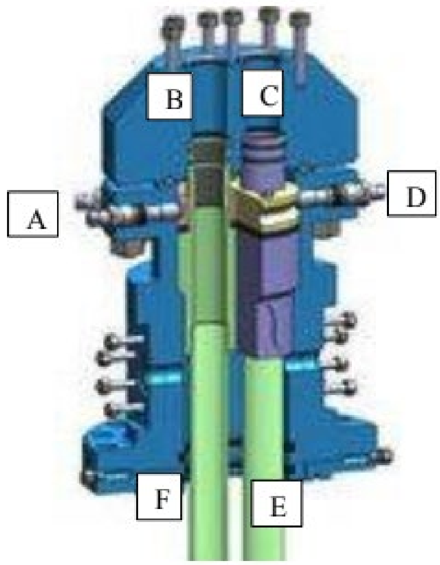

Figure 25. Example of Dual Completion Head

The last evaluated option took a drilling approach to designing the wellhead system. Instead of using a traditional wellhead and hanger system normally seen in the previous two options, this option uses an annular BOP and casing spools. In this system, the 11.625-inch casing head already installed to the top of the casing and wellbore will still be used. On top of the casing head, two casing spools with two flanges each (**Figure 28**) will be installed. One casing spool will allow for the pressurization and temperature variances of the fluid in the wellbore. The other casing spool will have one flanged connected to a pressure gauge to monitor the surface pressure of the well with the other flange closed. On top of the casing spools the annular BOP will be installed (**Figure 29**). Because the annular BOP uses a bag to hydraulically seal the hole, it should close around all associated cables and equipment without damaging them. A 10- to 15-foot piece of

2.375-inch production tubing will be used with the annular BOP to prevent damage to the bag. While the BOP can hydraulically close without anything equipment running through it, it will damage the bag to the point of it needing to be replaced before the BOP can be used again. Using the piece of production tubing will prevent, or at least minimize, any damage that would occur from the bag having to close so tight without it could close around. It can be seen in Figure 4 that even in the demonstration of the BOP in the shop, a piece of tubing was still used to prevent damage of the bag. The annular BOP has a rating of being able to withstand up to 5,000 psi at the surface which is well above the surface pressure criteria. Without the restriction of hole size seen in a hanger system, it was determined to evaluate the use of a single cable with 7 conductors for the sensor plus the mono-conductor cable previously described for the reference gauge for a total of two cables being used for the experiment.

Figure 26. Casing Spool

Figure 27. Annular BOP

At first glance, the dual completion option was promising as it allowed for cables to pass easily from the wellbore to the surface through one side of the wellhead. However, sealing around the cables and the ability to keep the wellbore pressurized during testing would not be possible; thus, failing to meet some of the criteria required for testing. Next, the fit-for-purpose design by TechnipFMC and casing spool and BOP system both meet all the criteria listed. As a result, these two options were compared on availability and economy. Because the TechnipFMC solution was designed specifically for this project, the wellhead and hanger system were going to have to be fully engineered and machined for the project. These facts made the availability hard as it could not be used until it was finished being produced, and the cost was going to be significantly higher due to the engineering and machining it would take to develop it for field use. Having a wellhead system designed for a one-time project on a non-producing well also made it difficult to justify the cost to have this system developed. The casing spool and annular BOP design, though, could easily be rented through a 3rd party vendor or service provider making it readily available and cost efficient due to only costing money for the days they were being used. As a result, it was decided the casing spool and annular BOP system would be the best fit for this project.

4.3.3 Inserting the Sensor Downhole

After the Quest team has removed the plug, swabbed the hole, and rigged down, the wellhead system will be installed. Three methods of installing the sensor downhole were evaluated. These methods included i) free fall or suspension of the sensor using the cable, ii) installing sensor inside a string of production tubing, and iii) mounting and lowering the sensor using sucker rods installation. Due to the selected wellhead system, the wellhead must be installed prior to any of the three methods being used to install the sensor. The sensor and associated equipment must be installed through the wellhead system so the annular BOP can close around it. A set of criteria was created to evaluate each of the three methods for sensor installation for best fit.

<u>Sensor Displacement Criteria</u>

a) Weight placed on cable connections and damage caused.
b) Movement of sensor within wellbore.
c) Sealing the wellbore for pressurization.

**If multiple sensor displacement methods meet all of the criteria listed above, then those methods will be evaluated on the availability and economics for best fit. **

The first option for inserting the sensor and reference gauge into the hole is to let them hang freely and be suspended by their respective cables at a depth of 3,000 feet. This option requires the least amount of material and effort to lower the sensor into the wellbore. However, it also allows for the sensor and reference gauge to freely move around the wellbore during installation and testing. Horizontal movement could cause damage to the sensor by colliding with the casing or reference gauge. Vertical movement would change the depth and cause different pressure readings than the ones expected during testing. In addition, the weight of the sensor could cause damage to the many electrical connections needed to transmit the signal to the surface as it would be dependent on those connections.

The second option involves 2.375-inch production tubing to lower the sensor into the wellbore. Two different strategies were considered with the tubing. The first approach was to strap or weld the sensor to the outside of the first joint in the hole. This would allow the cables to be strapped to the outside of the tubing and run through the BOP to the surface. Because the housing of the sensor has an outer diameter of 2.875 inches, placing it on the outside of the 2.375-inch production tubing would give a total outer diameter of 5.25 inches. The second tactic using the tubing casing was to have the sensor installed on the inside of the first joint. A hole large enough for the cables to exit the tubing would be drilled somewhere just above the placement of the sensor. This hole would allow the tubing to be sealed on the inside above the cables to prevent leakage and allow pressurization of the wellbore while also permitting the cables to run on the outside of the tubing through the BOP to the surface.

The third option is comparable to the second option, but it uses sucker rods to lower the sensor instead of production tubing. 0.75-inch sucker rods would be used. The sensor would be strapped to the first sucker rod in the hole with the associated cables strapped along the sucker rod string to the surface. As previously described, a 10- to 15-foot piece of 2.375-inch production tubing will be attached to the top sucker rod at the surface. The piece of tubing will be capped inside the hole to prevent leakage and keep pressurization during testing. The BOP will close around the piece of production tubing instead of just the sucker rod to prevent damage when opening and closing the bag of the BOP.

While it would be the cheapest option, the cable suspension method was deemed inefficient due to the chance of horizontal and vertical movements plus the stress it would be purely on the electrical connections within the sensor. The chance of the electrical connections coming undone downhole would be detrimental to performing a successful test. The first production tubing tactic was also determined to be an inadequate way of installing the sensor due to the amount of room it would require downhole. The hole is cased with 7-inch casing meaning the inner diameter of the casing would be extremely close to the outer diameter of the tubing and sensor system of 5.25 inches. A tight squeeze when installing the equipment downhole could potentially damage the sensor beyond usage if it hits the casing wall too hard. Thus, this method with the production tubing was also considered an unsatisfactory way of installing the sensor downhole.

The second production tubing approach and sucker rod method were both evaluated to be efficient enough to install the sensor downhole. Neither style causes tension on the electrical connections of the sensor, takes too much space downhole, and would allow the wellbore to stay pressurized. As a result, both options were weighed against each other based on availability and cost. Currently, both are readily available locally and would just need to be purchased and picked up; however, purchasing 3,000 feet of sucker rods is significantly cheaper than 3,000 feet of production tubing Therefore, the sucker rod method was determined to be the most efficient option to installing the sensor downhole for testing.

4.3.4 Pressurizing the Well

A hot oiler truck provided by Quest through a 3rd-party vendor will be used to hydrostatically pressurize the well and create a temperature variance throughout testing. To create a cyclic system, the hot oiler truck will connect two flow lines to the bottom casing spool. On one side, the inlet flow line will be connected allowing water to be pumped into the wellbore. On the other side of the casing spool, an outlet flow line will be connected allowing water to leave the wellbore and circulate throughout the entire system and back to the hot oiler truck. The circulation will allow for the hot oiler truck to heat or cool the entire system. The top casing spool will have a pressure gauge connected to one valve while the other valve will be closed.

A total of four tests will be run on the sensor. The first 3 will be cyclic pressure tests where the pressure at 3,000 feet will be roughly 1.5x the hydrostatic pressure of water. Using the pressure gradient for water of 0.433 psi/ft, the hydrostatic pressure at a depth of 3,000 feet is p = 0.433 psi/ft * 3,000 ft = 1,300 psi. Thus, the pressure needed to run the tests is p = 1.5 * 1,300 psi = 1,950 psi. By taking the difference of the normal hydrostatic pressure and 1.5x the normal hydrostatic pressure, the pressure at the surface would read p = 1,950 psi – 1,300 psi = 650 psi. Therefore, the pressure gauge attached to the top casing spool should read 650 psi when the well is pressurized. The fourth and final test will be an extended pressure test and will be pressurized to the 1.5x hydrostatic pressure and left for approximately two weeks to test the drift on the sensor over time.

4.3.5 Tearing Down and Plugging the Hole

Once the tests have commenced, clearing of the hole will begin. To begin this process, the hot oiler will depressurize the hole by removing all excess water and returning the pressure to the original open hole pressure before the hole was sealed. After the hole has been depressurized, the workover rig will be brought back and connect to the sucker rod system allowing the BOP to be opened. Next, the workover rig will be able to extract all the equipment placed downhole. Once the hole is cleared, the wellhead system can be detached from the casing head and a new cement plug will be placed in the wellbore. A test will be run to ensure proper plugging. After the hole is cleaned and plugged, the OU team will retain the wellhead system, sucker rods and tubing, the reference gauge, the sensor, and wires associated to operate the gauge and sensor. The 3rd party vendors will remove the remaining products and tools they provided from the area.

Chapter 5. Field Test Results

This chapter outlines the activities and the results from the field test.

5.1 Field test timeline

The detailed testing schedule is shown in Table 1.

Table 5. Timeline of the field test at research wellbore (Quest).

Task	**Details**	**Start Date**	**Days to Complete**
Sensing system preparation	Making sure all the sensors and instruments are ready for delivery to the field.	12-Sep	7
Wellbore preparation	Drill out the plug, swab and clean the hole to a depth of 3,100 ft.	19-Sep	28
Sensor installation	Mounting and lowering the sensor downhole.	24-Oct	3
Pressurizing test	Pressurizing the wellbore by pumping water to test the dynamic response of the sensor	27-Oct	1
Drift test	Continuously logging the sensor readings for over 2 weeks to test the sensors long term drift	27-Oct	15
End of test	Pulled out the sensors from downhole.	11-Nov	7

5.2 Sensing system preparation

Starting near the beginning of September, the sensor cables, sensor housing, data acquisition system and software, and the reference sensor were all tested for the field. We packaged the sensors with their respective cables by connecting them carefully before delivering to the testing facility.

5.3 Wellbore preparation

Wellbore preparation was planned to begin on September 19th, 2022. In Section 4.3.1, it was mentioned that Quest would drill out a cement plug in the wellbore. This plug was believed to roughly be 300 ft in total length. However, after several days of attempting to drill out the plug with a workover rig (**Figure 30 (a))**, it was realized the previous company who used the wellbore cemented roughly 3,000 ft of the wellbore. As a result, the workover rig was released from the project due to the length of the cement plug. Once Quest was able to locate a drilling rig, it was moved onto location to drill the remainder of the plug out to a depth of about 3,200 ft. This mishap added about a month's time to complete plus cost for the higher day rate and operational cost for a drilling rig compared to the workover rig. The drilling rig is shown in **Figure 30 (b)**. On October 21st, 2022, Quest and the drilling team completed the wellbore cleaning, marking its readiness for sensor installation.

(a) (b)

Figure 28. (a) Workover rig, (b) Drilling rig.

5.4 Sensor installation

5.4.1 Wellbore Schematic

The schematic of the test system is shown in **Figure 31**.

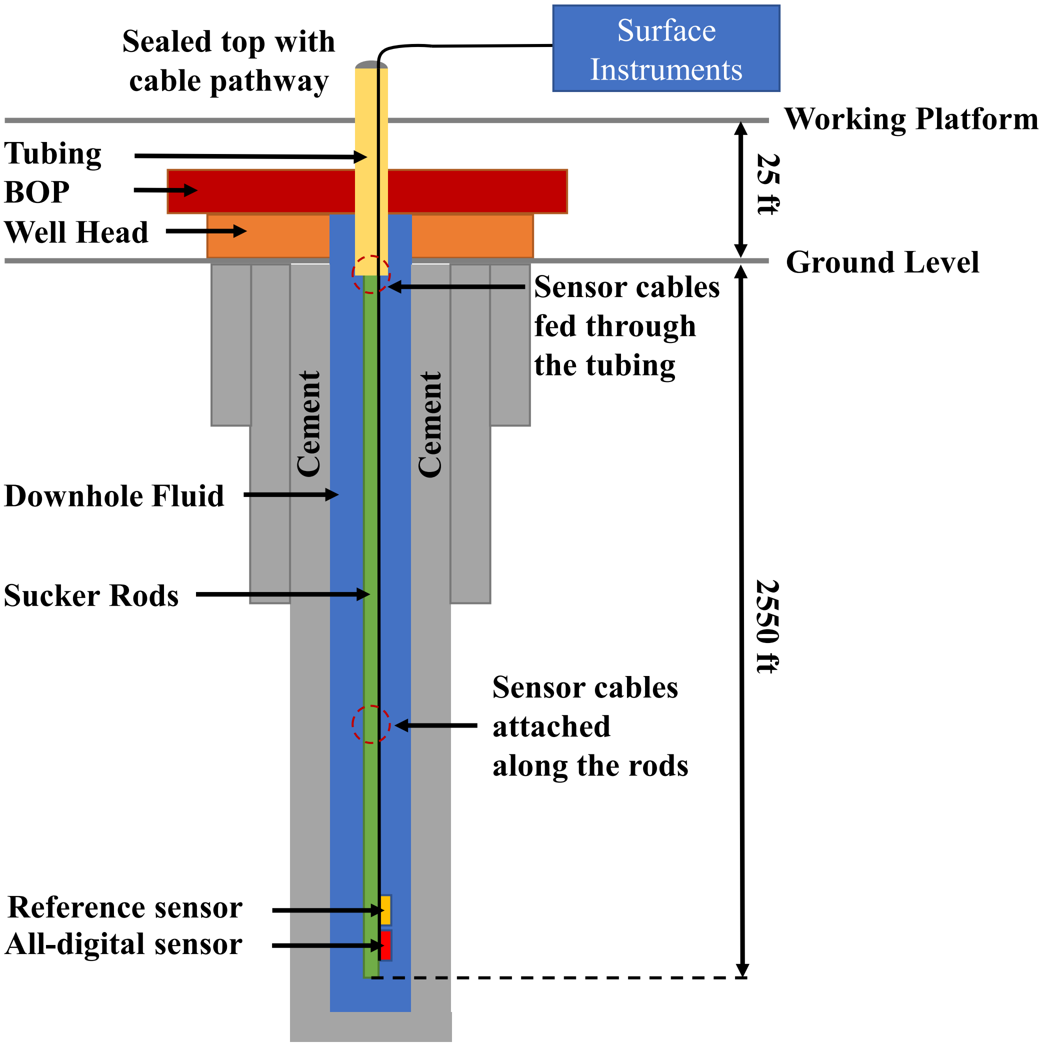

Figure 29. The schematic of the test system. BOP, blowout preventor.

5.4.2 Lowering down the sensor

Figure 30. The all-digital sensor and reference sensor were connected to their cables.

The sensor systems were delivered to Quest Drilling on pallets connected to spools of their respective cable as shown in **Figure 32.** The all-digital sensor and reference sensor were strapped to the second sucker rod inserted into the wellbore. Zip-ties and metal band clamps were used to tie the sensor and the cable onto the rods. **Figure 33** describes the sensor lowering process. 3 band clamps were used to fix the all-digital sensor to the sucker rod, and 4 band clamps were used with the reference sensor. After putting on the band clamps, waterproofed tape was applied around the outside of the sensor to ensure there would be no leakage around the cable connections. The cables were attached to each rod using at least three zip-ties per rod.

Because the downhole environment was unstable, only 104 sucker rods were used to lower the sensors downhole. After further evaluation, the top 2 rods were taken back out and laid down for the tubing connection needed to secure the wellhead for a total of 102 sucker rods in the hole. Thus, the depth of the sensor was about 2550 ft. The top end of sucker rod was connected to a capped piece of production tubing. Both cables passed through the cap via two holes drilled in the top of the cap on the production tubing. J-B Weld was exploited to seal the tubing cap around the cables as shown in **Figure 34**. A 24-hour cure time was required before performing the pressure tests. The two cables were connected to the data acquisition system placed in the doghouse. The data acquisition setup is shown in **Figure 35**. There were no issues with the data acquisition systems reading the sensors during the entire process of installation into the wellbore.

(a) (b) (c) (d) (e) (f)

Figure 31. (a) The all-digital sensor was attached to the suck rods by three band clamps. (b) and covered by waterproofed tape. (c) The reference sensor was attached to the suck rods by four band clamps and (d) covered by the waterproofed tape. (e) Two cables were fixed to the sucker rods using zip-ties. (f) A production tubing was placed on the last rod.

Figure 32. Tubing cap with the cable pass through.

Figure 33. Surface sensor reading instruments setup.

The pressure reading was recorded every 10 rods lowered into the wellbore, or roughly every 250 ft. It was observed the measured pressure increased as the depth into the wellbore increased. In addition, the measured pressure matched accurately with the reference sensor reading at roughly 2,550 ft. The results are shown in the **Figure 36**.

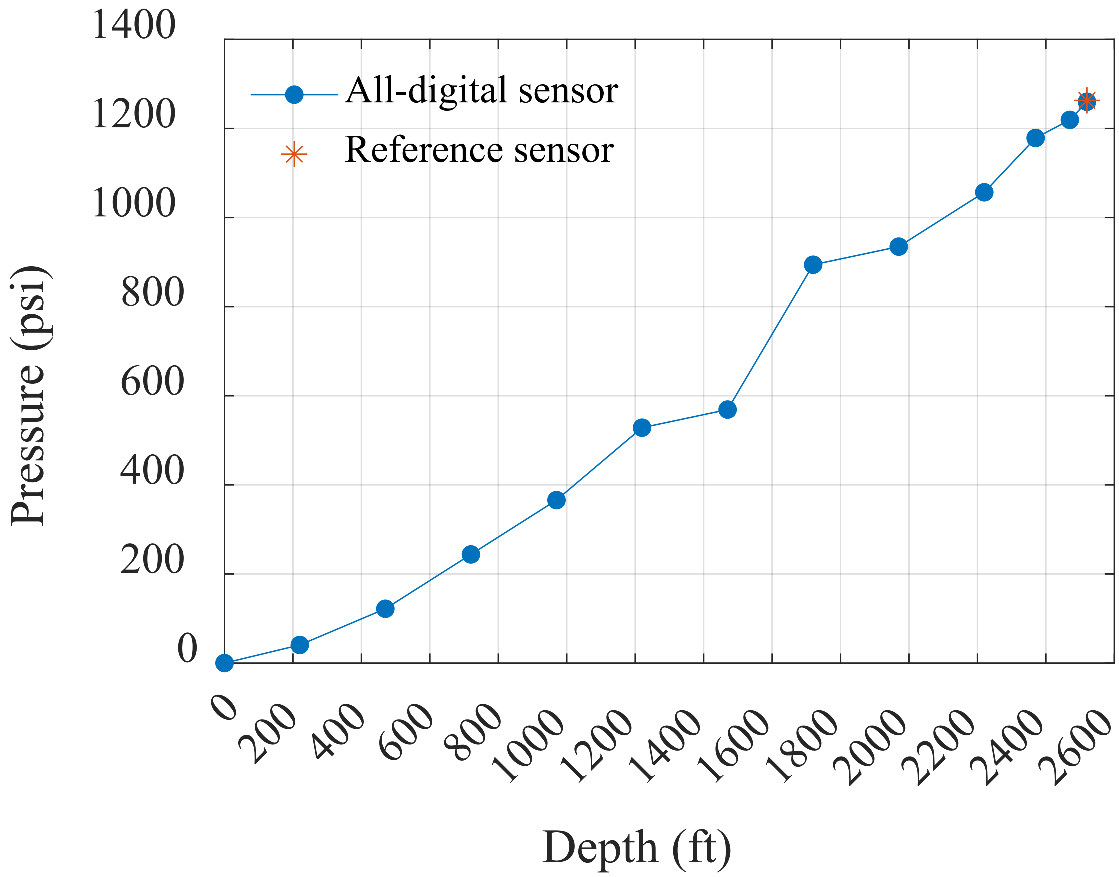

Figure 34. Testing result when lowering downhole

5.5 Pressurizing test

Figure 37 shows the pump truck used to pump water into the wellbore allowing pressurization of the hole and sensors. Because the measurement range of the all-digital sensor from the laboratory was 2,000 psi and the hydrostatic pressure of the sensor at 2,550 ft was about 1,260 psi, it was determined to only apply an additional 700 psi of pressure to the wellbore. However, during the pressuring process, it was found the maximum amount of additional pressure that could be achieved was around 300 psi which results in a downhole pressure of 1,600 psi. Curious to why a higher pressure could not be achieved, the inlet of the wellbore at ground level and the cable outlet on the working platform were checked for a leakage point. No leaks were found above the surface.

Thus, it was determined the leakage is occurring downhole either from the sensor system or wellbore itself. It was determined the sensor was holding properly and to continue testing.

Figure 35. Pump truck used for the pressuring test.

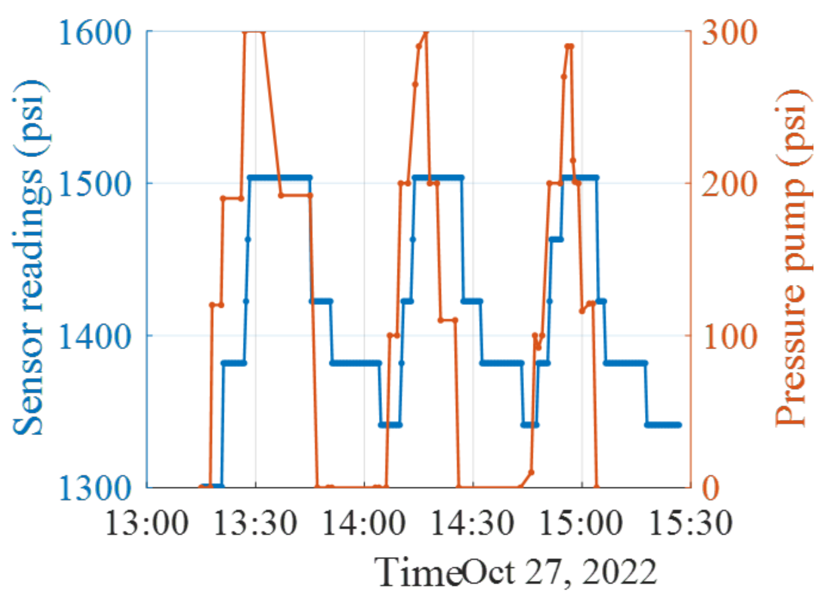

Figure 36. Pressurizing test

To test the fluidity of the all-digital sensor in a live environment, a step test was performed in increments of 100 psi from a surface pressure of 0 psi to 300 psi 3 separate times. After each increment or decrement step, the pressure was held for 2 minutes to see the pressure variance occur on the sensor. The changes in pressure with the all-digital sensor and at the surface can be seen in **Figure 38**. The blue line represents the all-digital sensor pressure while the orange line represents the surface pressure. The step tests prove the downhole sensor can follow the pressure changes applied at the top of the wellbore. It is important to note the applied pressure has a maximum difference of 300 psi while the sensor only has 200 psi output difference. This could be explained by the 100-psi hysteresis of the downhole sensor observed in the laboratory.

5.6 Drift test

After the conclusion of the step test, a sensor drift test was conducted for about two weeks. The all-digital sensor readings remained stable for the duration of the two-week test. While there was a couple of pressure drops at the end of the test, it was determined to not be a malfunction of the sensor and possibly caused by precipitation of the downhole fluid. There is no leakage of the sensor housing, and the sensor was still functioning properly after the test once removed from the wellbore.

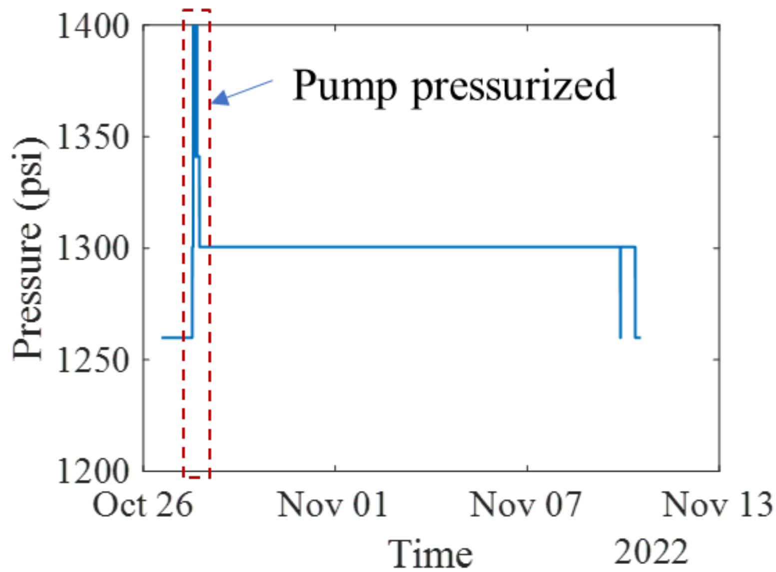

Figure 37. long-term stability test

Chapter 6. Conclusions

In this thesis, we conceptualized, developed, and verified an innovative sensor system accompanied by a designed sensor housing. The work required crafting the housing from its inception, progressing through the stages of fabrication, and ultimately subjecting the sensor-housing ensemble to comprehensive testing within both controlled laboratory environments and real-world research wellbores. The following main conclusions can be drawn from this work.

A 23-inch long, 2.875-inch diameter and 0.434-inch wall thickness sensor housing was designed with a high-strength 1045 carbon steel, 1.50 inches and a pitch of 0.15 inches for a total of 10 revolutions and it's design was verified with finite element analysis. by subjecting the sensor housing component to a requisite pressure of 10,000 psi. The housing demonstrated its capacity to withstand this pressure thru its individual parts and as a full assembly in lab tests and field tests.

The sensor showed a linear pressure response in the laboratory test range of 0-2000psi pressure. A consistent 100 psi hysteresis was seen from the pressure loading and unloading phase. This is expected to be caused by friction in the digital encoder. A successful design for installation was created and executed using a annular BOP as pressure control at the surface. The BOP bag pressing on the pipe created a low cost option for pressure control for a one-off test design.

Despite encountering challenges during the testing phase, such as the tough removal of the wellbore plug, and fluid losses when well was pressurized we managed to successfully install and test and confirm the performance of both the sensor and its housing under conditions up to 2,000 psi and and managed to successfully achieve a pressure increase of 300 psi for the purpose of sensor testing. Our obtained results aligned well with those of the reference sensor.

Following the testing phase, we removed the sensor and proceeded to inspect the housing for any potential signs of leakage. The absence of any leaks, along with the consistent, rapid readings, serves as strong evidence of the highly successful overall design.

This work shows a promise for the all-digital pressure sensor system. For the future the hysteresis needs to be addressed and reduced and the overall pressure sensor diameter needs to be reduced before commercially developed.

References

Bateman, K., Molenaar, M. M., & Brown, M. D. 2013. Lessons Learned from Shell's History of Casing Conveyed Fiber Optic Deployment. Presented at the SPE Unconventional Resources Conference Canada, Calgary, Alberta, Canada, November 5-7, 2013. https://doi.org/10.2118/167211-MS.

Bense, V., Read, T., Bour, O. et al. 2016. Distributed Temperature Sensing as a downhole tool in hydrogeology. *Water Resources Research* **52** (12): 9259-9273. http://dx.doi.org/10.1002/2016wr018869.

Costello, C., Sordyl, P., Hughes, C. et al. 2012. Permanent Distributed Temperature Sensing (DTS) Technology Applied In Mature Fields: A Forties Field Case Study. Presented at the SPE Intelligent Energy International, Utrecht, The Netherlands, March 27-29, 2012. https://doi.org/10.2118/150197-MS.

Davis, J. R. 1997. *ASM Specialty Handbook: Heat-Resistant Materials*, . : ASM International.

Halliburton. 1995. *Halliburton Cementing Tables*, Halliburton Company.

Halliburton. 2020. “Fiber-Optic Sensing Technologies for Well Monitoring to Reservoir Management.” Retrieved January 20, 2022, from www.halliburton.com.

Halliburton. 2023. *eRedbook*, Retrieved January 20, 2022, from www.halliburton.com.

Holley, E. H., and Kalia, N. 2015. Fiber-Optic Monitoring: Stimulation Results from Unconventional Reservoirs. Presented at the Unconventional Resources Technology Conference, San Antonio, Texas, 20-22 July, .

Joe, Hang-Eun, et al. 2018. "A Review on Optical Fiber Sensors for Environmental Monitoring." *International Journal of Precision Engineering and Manufacturing-Green Technology* 5(1): 173-191.

Koelman, Vianney, J. V., Lopez, J. L. et al. 2011. "Fiber Optic Technology for Reservoir Surveillance." Presented at the International Petroleum Technology Conference, International Petroleum Technology Conference.

Marcuccio, S., Flygare, J., & Konopczynski, M. 2015. “Application of Pressure-Monitoring Data in Land-Based Unconventionals.” Presented at the SPE/CSUR Unconventional Resources Conference.

Mateeva, A, et al. 2014. "Distributed Acoustic Sensing for Reservoir Monitoring with Vertical Seismic Profiling." *Geophysical Prospecting* 62(4): 679-692.

Na, Y. 2024. “Validation and Field Testing of an All-Digital Pressure Sensor for Permanent, Distributed Downhole Measurements.” Ph.D. Dissertation, University of Oklahoma, OK.

Qi, B., Pickrell, G. R., Zhang, P., et al. 2002. “Fiber Optic Pressure and Temperature Sensors for Oil Downhole Application.” Presented at the Fiber Optic Sensor Technology and Applications 2001.

Schenato, Luca. 2017. "A Review of Distributed Fibre Optic Sensors for Geo-Hydrological Applications." *Applied Sciences* 7. 896..

McMaster-Carr. 2023. Steel Rods, *McMaster-Carr*. https://www.mcmaster.com/products/steel-rods/diameter~2-7-8/ accessed July 2023.

Tardy, Jacques, P. M., Chang, F. F., et al. 2011. "Determining Matrix Treatment Performance from Downhole Pressure and Temperature Distribution: A Model." Presented at the International Petroleum Technology Conference, International Petroleum Technology Conference.

Wise, J. 2021. Numerical Simulations of Wellbore Cement Sheath Microannuli Leakage in Gulf of Mexico Wells. MS Thesis. University of Oklahoma, Norman, OK.

Xiao, H. 2024. Final Scientific Report. *All-digital Sensor System for Distributed Downhole Pressure Monitoring in Unconventional Fields.* U.S. Department of Energy (DOE) and National Energy Technology Laboratory sponsored project DE-FE0031781.

Xiao, H. and Zhu, W. 2019. All-Digital Sensing Device and Implementation Method. 10,402,709.